

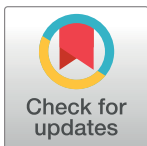
RESEARCH ARTICLE

Inferring causal pathways among three or more variables from steady-state correlations in a homeostatic system

Suraj Chawla, Anagha Pund, Vibishan B., Shubhankar Kulkarni, Manawa Diwekar-Joshi, Milind Watve^{*}

Biology, Indian Institute of Science Education and Research, Pashan, Pune, Maharashtra, India

* milind@iiserpune.ac.in



Abstract

Cross-sectional correlations between two variables have limited implications for causality. We examine here whether it is possible to make causal inferences from steady-state data in a homeostatic system with three or more inter-correlated variables. Every putative pathway between three variables makes a set of differential predictions that can be tested with steady state data. For example, among 3 variables, A, B and C, the coefficient of determination, r_{AC}^2 is predicted by the product of r_{AB}^2 and r_{BC}^2 for some pathways, but not for others. Residuals from a regression line are independent of residuals from another regression for some pathways, but positively or negatively correlated for certain other pathways. Different pathways therefore have different prediction signatures, which can be used to accept or reject plausible pathways using appropriate null hypotheses. The type 2 error reduces with sample size but the nature of this relationship is different for different predictions. We apply these principles to test the classical pathway leading to a hyperinsulinemic normoglycemic insulin-resistant, or pre-diabetic, state using four different sets of epidemiological data. Currently, a set of indices called HOMA-IR and HOMA- β are used to represent insulin resistance and glucose-stimulated insulin response by β cells respectively. Our analysis shows that if we assume the HOMA indices to be faithful indicators, the classical pathway must in turn be rejected. In effect, among the populations sampled, the classical pathway and faithfulness of the HOMA indices cannot be simultaneously true. The principles and example shows that it is possible to infer causal pathways from cross sectional correlational data on three or more correlated variables.

OPEN ACCESS

Citation: Chawla S, Pund A, B. V, Kulkarni S, Diwekar-Joshi M, Watve M (2018) Inferring causal pathways among three or more variables from steady-state correlations in a homeostatic system. PLoS ONE 13(10): e0204755. <https://doi.org/10.1371/journal.pone.0204755>

Editor: Massimiliano Ruscica, Università degli Studi di Milano, ITALY

Received: March 6, 2018

Accepted: September 13, 2018

Published: October 11, 2018

Copyright: © 2018 Chawla et al. This is an open access article distributed under the terms of the [Creative Commons Attribution License](https://creativecommons.org/licenses/by/4.0/), which permits unrestricted use, distribution, and reproduction in any medium, provided the original author and source are credited.

Data Availability Statement: All relevant data are within the paper, supporting information and previously published studies (ref 37-39).

Funding: This work was supported by Rajiv Gandhi Science and Technology Commission (RGSTC), Maharashtra State.

Competing interests: The authors have declared that no competing interests exist.

1. Introduction

1.1. Overview

In the field of biomedicine, the nature of causality, and the use of correlations as an evidence for causality are much debated [1–4]. There have been many attempts to develop sound methods to address questions of causal inference from correlational data which include Hill criteria

[5], path analysis [6–9] the use of instrumental variables [10], Granger causality [11], Rubin causal model [12], or additive noise models [13]. Hill criteria are a set of common sense criteria useful in avoiding misguided inferences. Path analysis generally assumes a direction of causality, usually directed acyclic paths, and while it is useful in determining the contributions of different causal pathways to a process or a resultant variable, its application to pathways with loops and cycles is difficult. Methods like Granger causality depend upon the assumption that the cause always precedes effect and that the variables show some degree of chaos or turbulence, so that there are notable events like sudden peaks in the variables that can be tracked using longitudinal data. In evolved systems in which predictive adaptive responses are possible, the assumption that cause always precedes effect is questionable. Another class of methods like Propensity Score matching based on the Rubin causal model works well to estimate the effect of a causal factor but does not take into account unobserved factors. The Rubin Causal Model also incorporates the structural equations model as it includes non-parametric forms [14,15]. Models like additive noise can suggest the direction of the arrow of causality between two variables, but they require the assumption that either A causes B, or B causes A, without any confounding, looping or circularity [16,17].

More specifically, here we look at homeostatic systems which are extremely common in fields such as physiology. Homeostatic systems pose a unique problem for causal inferences. Causal inference can be based on time-series analysis with longitudinal data [18]. Longitudinal data are of little use however, if the time taken to reach equilibrium is smaller than the observational window, or if the system is already in a steady-state. Most homeostatic systems have negative feedback or some loop structures, because of which methods assuming acyclic causal paths or freedom from confounding are not applicable.

Although the use of correlations to infer causality is doubted, intervention experiments are generally taken as a convincing evidence of causality. However, causality in steady-state can be substantially different than causality in a perturbed-state and inferences from a perturbation experiment may not be applicable to steady-state causality. This necessitates a set of tools to infer causality in a steady state which is independent of perturbing interventions. We argue in this paper that it is possible to infer causal relationships among three or more variables from cross-sectional data in a homeostatic system in which the variables and their relationships are stable in time.

1.2. Motivation

Our motivation and the need for this tool came from some debated causal pathways in the pathophysiology of type 2 diabetes (T2D). According to the classical view, obesity-induced insulin resistance is primary, and rise in insulin levels is a compensatory response to insulin resistance, mediated by raised levels of glucose [19,20]. This is contested [21], with increasing evidence suggesting that hyperinsulinemia precedes insulin resistance [22–26]. There is also evidence of neuronal signals affecting insulin production on the one hand, and controlling glucose production by the liver partly independent of insulin on the other. Therefore, the causal relationship between insulin resistance, hyperinsulinemia and hyperglycemia needs to be re-examined (reviewed by [21]).

Elucidation of the causal pathway for a pre-diabetic or diabetic state is critical at the clinical level because the current approaches to medication are designed assuming one particular pathway, and have largely failed to cure diabetes. If it is possible to determine causality reliably, it can potentially change diabetes medicine. It has long been recognized that levels of glucose and insulin are under homeostatic control, and that fasting is a steady state [27–30]. With substantial data available on fasting levels of glucose and insulin from different populations, along

with many other variables, a tool for inferring causality from a set of inter-correlated steady-state variables would help understand, and thereby better control, T2D.

Beyond the specific problem of causality in pre-diabetes, a set of methods that can help infer causality from steady-state data will find a large number of applications, not only in physiology and disease, but in many other areas of science. Although our investigations began with the pathophysiology of diabetes, the emerging principles are generalizable and valuable for inferential statistics in general.

1.3. Organization of the paper

Since the question addressed here and the approach suggested is complex we have organized the paper in the following sections. Section 2 describes the underlying principle and basic assumptions and spells out the nomenclature used in the rest of the paper. Section 3 details the development of the theoretical framework that is the central element of this work. We discuss first, possible alternative causal pathways between three inter-correlated variables, followed by the distinction between causal and regression equations that will underlie the subsequent analysis. In the interest of brevity, in the main text we restrict ourselves to reproducing only the final analytical prediction for each pathway, classified into acyclic and cyclic pathways, adding a few lines where pathway-specific predictions necessitate discussion. Complete proofs and derivations are instead relegated to the supplementary text. Section 4 discusses the testing of pathway predictions against suitable null hypotheses, and Section 5 describes findings regarding the sensitivity and robustness of the analytical predictions derived so far. Section 6 provides a general description of potential applications of the above theoretical framework. Section 7 encompasses a comprehensive demonstration of application of the framework to a real-life question in diabetes research. We first discuss in some detail, the current view on causal factors in diabetic and pre-diabetic states, before moving on to the dual feedback model that forms the main hypothesis to be tested. We analyze the system according to the methods detailed in previous sections, and present several novel observations along with their significance to diabetes research.

2. Methods

2.1. Overview

We show here that when three inter-correlated variables are considered together with two or more causal arrows connecting them to make a causal pathway, each of the possible pathways makes a set of differential predictions by which the pathways can be differentiated from each other. Our approach to develop a method of inferring causality from cross sectional regression correlation parameters comprises following steps:

Development of a theoretical framework-

- i. We first list the perceived possible hypothetical causal pathways among three variables.
- ii. For each pathway, we write a set of causal equations arising out of the hypothetical pathways. Steady-state solutions of these equations lead to a set of four general, and a few pathway-specific predictions. Each pathway therefore has a unique combination of such predictions or a prediction signature by which it can be differentiated from other pathways.

Testing the pathways by simulations-

- i. We test, using simulated data generated from assumed causal pathways, the conditions under which the predictions can be used to accept or reject a pathway reliably.

- ii. Based on these results, we suggest ways of handling multivariate data and infer causal networks among them.

Demonstration of a specific example-

- i. We apply this logic to the specific case of pre-diabetes to examine the pathway classically thought to give rise to this condition.

2.2. Baseline assumptions and nomenclature

We consider three variables labelled A, B and C. Additional variables if needed to describe a pathway will be labelled X, Y and so on. All causal relationships represented by a single arrow are assumed to be linear, and all primary input variables are assumed to be normally distributed. In a given operation, the slopes of causal pathways are assumed to be constant; the errors in causal pathways are assumed to be distributed normally, with means of zero and a constant standard deviations, and no covariance with each other. We assume that the errors are caused by variation in individual responses, and that a given individual's response is consistent in time sufficiently long to reach a steady state. Thus, the errors are randomized over the population, but for a given individual, they are constant in time. We assume no measurement error in the baseline models. Since all our predictions are related to correlation coefficients and regression slopes, we will ignore the intercepts for the sake of simplicity in deriving many of the predictions.

3. Development of a theoretical framework

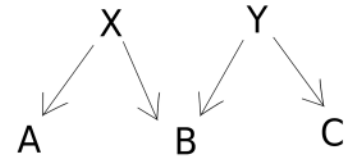
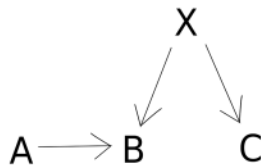
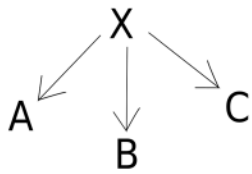
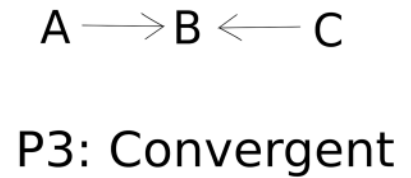
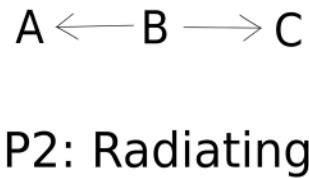
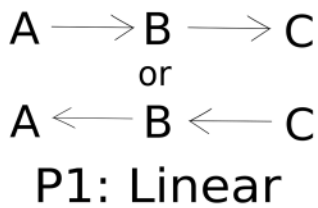
3.1. The possible pathways

A variety of cyclic and acyclic pathways can exist in three variables. Fig 1 shows the simple primary pathways that are possible, and more can certainly be constructed by combinations of the primary pathways. It is also possible to consider permutations of the three variables; for example, the linear pathway among three variables can itself be written in six different ways. Here, we restrict to the primary pathways assuming a fixed sequence of the three variables denoted by A, B and C. The principles that we derive from this set of primary pathways can be extended to more complex pathways.

3.2. Causal equations versus regression equations

Based on hypothesized pathways, we can write specific causal equations for each. The causal equations are derived from the hypothesized pathway, while the regression equations can be obtained from the given cross-sectional data using regression and correlation analysis. Our causal equations are similar to the structural equations of [15]. However, they differ in their interpretation and treatment. In structural equations, the left hand terms are effects and right hand terms are causes, and the two cannot be algebraically transferred without changing causal interpretations. In our approach, after finding equilibrium solutions, we can carry out algebraic operations freely in order to obtain testable predictions. The parameters of the regression equation are not necessarily identical to those of the causal equations (Table 1). For example, for a hypothesized pathway $Y = mX + C$, m is the causal slope, while the regression slope would be underestimated if there is post-effect variability in X [31], and such a bias in the slope is important in making and testing predictions. In the following section, we show that the parameters of causal equations hold pathway-specific relationships with the parameters of regression equations based on which, pathway-specific predictions about the regression correlation parameters can be made.

Acyclic pathways



Cyclic pathways

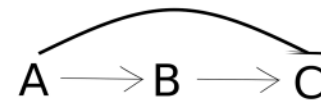
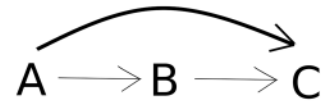
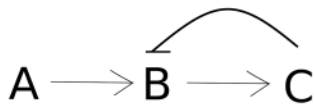
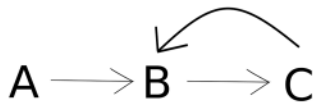


Fig 1. Possible primary causal pathways between three variables. More complex pathways can be visualized by combinations of the primary ones.

<https://doi.org/10.1371/journal.pone.0204755.g001>

For ensuring steady-state, we assume that a given variable has a rate of formation/increase and a rate of degradation/decrease. If the rate of degradation is positively dependent, or the rate of formation negatively dependent on the standing level, then the variable invariably reaches a steady state determined by the set of input parameters. Such steady states are characteristic of homeostatic systems, and this principle is central to our methods.

For example, in a linear pathway $A \rightarrow B \rightarrow C$, $\frac{dB}{dt} = m'_1A - d_1B$ and $\frac{dC}{dt} = m'_2B - d_2C$. At a steady-state the net change in any variable is zero. Therefore, the steady-state levels of B and C will be $B = \frac{m'_1}{d_1}A = m_1A$ and $C = \frac{m'_2}{d_2}B = m_2B$ respectively.

In simple cases, we need not explicitly include the rates of degradation in the equations but directly use parameters, m_1 and m_2 . For pathways involving loops and feedback, the relationships between variables are more complex, and therefore necessitate the use of degradation constants in the causal equations for ensuring steady-states.

Causal and regression parameters can be analytically related, and these relationships allow the formation of regression-based predictions for each pathway based on the known relationships between the corresponding causal parameters. Here, we put the two together and describe four general predictions across all pathways and formulate a null hypothesis for each. In addition, there are certain pathway specific predictions that will be discussed along with the description of the corresponding pathway. The four general predictions are:

1. Whether r^2_{AC} can be estimated from the product of r^2_{AB} and r^2_{BC} .
2. Whether slope M_{ca} can be estimated from the product of the slopes M_{ba} and M_{cb} .
3. Whether the residuals of the regression of B on A (E_{ba}) are correlated with those of C on B (E_{cb}): The errors or residuals in a regression are assumed to be random independent errors. However, we will show below that if there are loops, convergent or confounding elements in a pathway, E_{ba} and E_{cb} do not remain independent. Based on the nature of dependence between E_{ba} and E_{cb} , presence of, and possible nature of the loops and convergence can be inferred.
4. a. Whether correction for A improves or reduces the correlation of B with C , i.e. whether $r^2_{E_{ba}C}$ is greater or lesser than r^2_{BC} .
 b. Whether the extent to which $r^2_{E_{ba}C}$ is greater or lesser than r^2_{BC} can be predicted by r^2_{AB} .

Table 1. List of abbreviations used.

Abbreviation	Term	Remarks
A, B, C	Test variables	We have access from data
$\bar{A}, \bar{B}, \bar{C}$	Mean of A, B and C respectively	We calculate from data
X, Y	Unknown variables	Which affect test variables. We do not have access to these from data.
M_{ij}	Slopes of regression of i on j	e.g. M_{ba} is calculated as $M_{ba} = \frac{cov(B,A)}{var(A)}$
K_{ij}	Intercept of regression of i on j	e.g. K_{ba} is calculated as $K_{ba} = \bar{B} - M_{ba}\bar{A}$
E_{ij}	Residuals of regression of i on j	e.g. E_{ba} is calculated as $E_{ba} = B - M_{ba}A - K_{ba}$
r_{ij}	Correlation coefficient between i and j	e.g. r_{ij} is calculated as $r_{ij} = \frac{\sum e_i e_j}{\sqrt{\sum e_i^2} \sqrt{\sum e_j^2}}$
m_1, m_2, m_3	Slopes in causal equations including the degradation rates	We do not have access to these in data
e_1, e_2, e_3	Error distribution in causal equations, assumed to be normal with mean zero and standard deviations sde_j etc.	These are post-effect errors of the causal relationships which may get incorporated in pre-effect errors of a subsequent effect
e_a, e_b, e_c	Net variability in A, B and C	e.g. e_a is calculated as $e_a = A - \bar{A}$
k_1, k_2	Intercepts in causal equations	
d_1, d_2	Degradation /destruction rate constants in causal equations	Especially necessary in cyclic pathways

Parameters of causal equations are denoted by small letters and those of regression equations by capital letters.

<https://doi.org/10.1371/journal.pone.0204755.t001>

3.3. Pathway-wise analytical predictions

We will now state how each of the pathways makes specific predictions. For detailed formal proofs and derivations refer to [S1 Text](#). Each putative pathway makes specific predictions about the above and accordingly the causal relationships can be accepted or rejected. For example, whether obesity leads to altered lipid profiles that ultimately lead hyperinsulinemia is one possible pathway. In an alternative view hyperinsulinemia leads to obesity.

Pathways P1 to P5 represent acyclic pathways and P6 and P7 represents pathways with loops. In pathways with loops, since there is a cyclic dependence between the variables we begin with differential equations with variable-specific constant rates of disintegration that assure steady states. This set of equations is then used to derive equilibrium solutions.

3.3.1. Linear pathway (P1). The causal equations for a linear pathway are:

$$A = \text{input} = \dot{A} + e_a$$

$$B = m_1A + e_1 + k_1$$

$$C = m_2B + e_2 + k_2$$

Where e_a, e_1, e_2 are not correlated.

Regression parameters can be derived from the causal equations as follows. Since in regression of B on A , the slope = $\text{cov}(A, B)/\text{var} A$,

$$M_{ba} = \frac{\sum e_a e_b}{\sum e_a^2} = \frac{\sum e_a (m_1 e_a + e_1)}{\sum e_a^2} = \frac{m_1 \sum e_a^2}{\sum e_a^2} = m_1$$

$$M_{cb} = \frac{\sum e_c e_b}{\sum e_b^2} = \frac{\sum (m_2 e_b + e_2) e_b}{\sum e_b^2} = \frac{m_2 \sum e_b^2}{\sum e_b^2} = m_2$$

$$M_{ca} = \frac{\sum e_c e_a}{\sum e_a^2} = \frac{\sum (m_2 m_1 e_a + m_2 e_1 + e_2) e_a}{\sum e_a^2} = \frac{m_2 m_1 \sum e_a^2}{\sum e_a^2} = m_2 m_1$$

$$E_{ba} = e_b - M_{ba} e_a = m_1 e_a + e_1 - m_1 e_a = e_1$$

$$E_{cb} = e_c - M_{cb} e_b = m_2 e_b + e_2 - m_2 e_b = e_2$$

$$E_{ca} = e_c - M_{ca} e_a = m_2 e_b + e_2 - m_2 m_1 e_a = m_2 e_1 + e_2$$

For linear equations, there is little difference between the causal equations and regression equations ([Table 2](#)). The regression equations therefore become

$$B = M_{ba} A + E_{ba} + K_{ba} = m_1 A + e_1 + k_1$$

$$C = M_{ca} A + E_{ca} + K_{ca} = m_2 B + e_2 + k_2$$

$$C = M_{ca} A + E_{ca} + K_{ca} = m_1 m_2 A + (m_2 e_1 + e_2) + (m_2 k_1 + k_2)$$

Prediction R1: Based on the equations above and [Table 2](#), it can be shown that $r_{AC} - r_{AB}r_{BC} = 0$ (See [S1 Text](#) 'Linear pathway: Prediction R1: Proof 1' for formal proof).

Table 2. Relationship between the causal and regression equations for linear pathway.

Slopes	Errors
$M_{ba} = m_1$	$E_{ba} = e_1$
$M_{cb} = m_2$	$E_{cb} = e_2$
$M_{ca} = m_1 m_2$	$E_{ca} = m_2 e_1 + e_2$

<https://doi.org/10.1371/journal.pone.0204755.t002>

Prediction R2: From Table 2, it is obvious that the slope M_{ca} can be predicted from the product $M_{cb}M_{ba}$; $M_{ca} - M_{cb}M_{ba} = m_1 m_2 - m_2 m_1 = 0$.

Prediction R3: From Table 2, as there is no covariance between e_1 and e_2 , $r_{E_{ba}E_{cb}}^2 = r_{e_1 e_2}^2 = 0$

Prediction R4: For a linear pathway, it can be shown that

(a) $r_{BC} > r_{E_{ba}C}$ and further, (b) $\frac{r_{BC}^2 - r_{E_{ba}C}^2}{r_{BC}^2} = r_{AB}^2$

3.3.2. Radiating pathway (P2). The causal equations for this model would be

$$A = m_1 B + e_1 + k_1$$

$$B = input = \hat{B} + e_b$$

$$C = m_2 B + e_2 + k_2$$

Note that the relationship between causal parameters and regression parameters is substantially different in this pathway than the linear pathway (Table 3). For example, the causal slope is $\frac{1}{m_1}$, but there is an underestimation of the slope during regression which is predicted exactly by r_{AB}^2 .

However, this difference is not detectable from cross-sectional data alone. Therefore, the standard four testable predictions of this pathway remain similar to the linear pathway. We will describe later that differentiating between pathways P1 and P2 is possible using a different strategy.

Prediction R1: From Table 3, it can be shown that $r_{AC}^2 - r_{AB}^2 r_{BC}^2 = 0$.

Prediction R2: From Table 3; we see slope M_{ca} can be predicted from the product $M_{cb}M_{ba}$

Prediction R3: From Table 3, $cov(e_1, e_2) = 0 \therefore r_{E_{ba}E_{cb}}^2 = r_{e_1 e_2}^2 = 0$

Prediction R4: As formally shown in S1 Text ('Radiating pathway: Prediction R4: Proof 2'),

$$r_{E_{ba}C} < r_{BC} \text{ and } \frac{r_{BC}^2 - r_{E_{ba}C}^2}{r_{BC}^2} = r_{AB}^2$$

3.3.3. Convergent pathway (P3). The causal equations for this model would be

$$A = input = \hat{A} + e_a$$

$$B = m_1 A + m_2 C + e_1 + k_1$$

$$C = input = \hat{C} + e_c$$

where e_a, e_1 and e_c are uncorrelated.

Table 3. Relationship between the causal and regression equations for radiating pathway.

Slopes	Errors
$M_{ba} = \frac{1}{m_1} r_{AB}^2$	$E_{ba} = e_b (1 - r_{AB}^2) - \frac{1}{m_1} r_{AB}^2 e_1$
$M_{cb} = m_2$	$E_{cb} = e_2$
$M_{ca} = \frac{m_2}{m_1} r_{AB}^2$	$E_{ca} = m_2 e_b (1 - r_{AB}^2) - \frac{m_2}{m_1} r_{AB}^2 e_1 + e_2$

<https://doi.org/10.1371/journal.pone.0204755.t003>

Regression parameters derived from the causal equations are given in Table 4.

There are two pathway specific predictions for the convergent pathway, shared only by the different cause pathway. Firstly, we expect no correlation between A and C from this pathway, unless there are additional external pathways linking the two. The other unique feature of this pathway is that both A and C have independent causal influence on B. As a result, the effect of A adds to the error in the correlation between B and C and similarly, the effect of C contributes to the error in the correlation between A and B. As a result, $r_{AB}^2 + r_{BC}^2$ cannot be greater than 1, as shown below:

$$r_{AB}^2 + r_{BC}^2 = \frac{m_1^2 \sum e_a^2}{\sum e_b^2} + \frac{m_2^2 \sum e_c^2}{\sum e_b^2} = \frac{m_1^2 \sum e_a^2 + m_2^2 \sum e_c^2}{\sum e_b^2}$$

$\sum e_b^2 = m_1^2 \sum e_a^2 + m_2^2 \sum e_c^2 + \sum e_1^2$, so

$$r_{AB}^2 + r_{BC}^2 < 1$$

This prediction is so robust that if $r_{AB}^2 + r_{BC}^2 > 1$, the convergent pathway can be rejected right away. Since we assume A and C to be independent input variables we assume no correlation between them. However, if they are correlated due to some cause other than this pathway, only then $r_{AB}^2 + r_{BC}^2$ can be greater than 1.

Prediction R1: Unlike pathways P1 and P2, for the convergent pathway, it can be seen that $r_{AC}^2 - r_{AB}^2 \cdot r_{BC}^2 < 0$.

Prediction R2: Since the expected slope M_{ca} is zero, and both M_{ba} and M_{cb} are non-zero, their product is not a predictor of M_{ca} .

$$|M_{ca}| - |M_{cb} M_{ba}| < 0 \text{ as } |M_{ca}| = 0$$

Prediction R3: The correlation $r_{E_{ba}E_{cb}}$ is predicted to have the same sign as M_{cb} .

Prediction R4: It can be shown that (a) $r_{BC} < r_{E_{ba}C}$ and further, (b) $\frac{r_{E_{ba}C}^2 - r_{BC}^2}{r_{E_{ba}C}^2} = r_{AB}^2$.

Because this expression differs from R4 (b) of the earlier pathways, we can use a more generalized form for R4 (b) as $\frac{|r_{BC}^2 - r_{E_{ba}C}^2|}{\max(r_{BC}^2, r_{E_{ba}C}^2)} = r_{AB}^2$

3.3.4. Common cause pathway (P4). The causal equations for this model would be

$$X = input = \check{X} + e_x$$

$$A = m_1 X + e_1 + k_1$$

$$B = m_2 X + e_2 + k_2$$

$$C = m_3 X + e_3 + k_3$$

where e_x, e_1, e_2, e_3 are not correlated.

It needs to be noted that e_1, e_2, e_3 are important in defining this pathway. If e_2 is negligible the pathway approximates to the radiating pathway with B being the mediator between A and C.

Table 4. Relationship between the causal and regression equations for convergent pathway.

Slopes	Errors
$M_{ba} = m_1$	$E_{ba} = e_1 + m_2 e_c$
$M_{cb} = \frac{1}{m_2} r_{BC}^2$	$E_{cb} = e_c (1 - r_{BC}^2) - \frac{1}{m_2} r_{BC}^2 (m_1 e_a + e_1)$
$M_{ca} = 0$	$E_{ca} = e_c$

<https://doi.org/10.1371/journal.pone.0204755.t004>

Table 5. Relationship between the causal and regression equations for common cause pathway.

Slopes	Errors
$M_{ba} = \frac{m_2}{m_1} r_{AX}^2$	$E_{ba} = m_2 e_x (1 - r_{AX}^2) + e_2 - r_{AX}^2 \frac{m_2}{m_1} e_1$
$M_{cb} = \frac{m_3}{m_2} r_{BX}^2$	$E_{cb} = m_3 e_x (1 - r_{BX}^2) + e_3 - r_{BX}^2 \frac{m_3}{m_2} e_2$
$M_{ca} = \frac{m_3}{m_1} r_{AX}^2$	$E_{ca} = m_3 e_x (1 - r_{AX}^2) + e_3 - r_{AX}^2 \frac{m_3}{m_1} e_1$

<https://doi.org/10.1371/journal.pone.0204755.t005>

Similarly, at small e_1 , A becomes the mediator and at small e_3 , C becomes the mediator in a radiating pathway. For the way we have defined our predictions, e_2 is the most important error term in this pathway (Table 5).

One very special feature of this pathway is that qualitatively it is highly symmetric with respect to all the three variables A , B and C . This means that any permutation of them does not change the qualitative nature of any prediction. This can be used as a pathway specific prediction and a distinct signature for this pathway.

Prediction R1: It can be shown that $r_{AC}^2 > r_{AB}^2 \cdot r_{BC}^2$ for this pathway.

Prediction R2: $|M_{ca}| - M_{cb} M_{ba} > 0$

Prediction R3: The sign of the correlation $r_{E_{ba}E_{cb}}$ is decided by the signs of m_1 and m_2 . When both have the same signs $r_{E_{ba}E_{cb}}$ are negative and when they have opposing signs $r_{E_{ba}E_{cb}}$ is positive. In other words, the correlation multiplied by the sign of M_{ca} is always negative.

Prediction R4: For this pathway (a) $r_{E_{ba}C} < r_{BC}$ and (b) $\frac{r_{BC}^2 - r_{E_{ba}C}^2}{r_{BC}^2} r_{AB}^2$

3.3.5. Single different cause pathway (P5a). The causal equations for this model would be

$$X = input = \dot{X} + e_x$$

$$A = input = \dot{A} + e_a$$

$$B = m_1 A + m_2 X + e_1 + k_1$$

$$C = m_3 X + e_2 + k_2$$

where $e_x e_a e_1 e_2$ are not correlated. Regression parameters derived are in Table 6.

Two specific predictions of this pathway shared only by the convergent pathway (P3) are that $r_{AC}^2 = 0$ and that $r_{AB}^2 + r_{BC}^2 < 1$.

Prediction R1: $r_{AC}^2 - r_{AB}^2 \cdot r_{BC}^2 < 0$

Prediction R2: $|M_{ca}| < M_{cb} M_{ba}$

Prediction R3: The correlation $r_{E_{ba}E_{cb}}$ is predicted to have the same sign as M_{cb} .

Prediction R4: (a) $r_{BC} > r_{E_{ba}C}$ and further (b) $\frac{|r_{BC}^2 - r_{E_{ba}C}^2|}{\max(r_{BC}^2, r_{E_{ba}C}^2)} = r_{AB}^2$ is true.

Table 6. Relationship between the causal and regression equations for single different cause pathway.

Slopes	Errors
$M_{ba} = m_1$	$E_{ba} = m_2 e_x + e_1$
$M_{cb} = \frac{m_3}{m_2} r_{BX}^2$	$E_{cb} = m_3 e_x + e_2 - m_3 r_{BX}^2 \left(\frac{m_1 e_a}{m_2} + e_x + \frac{e_1}{m_2} \right)$
$M_{ca} = 0$	$E_{ca} = m_3 e_x + e_2 - m_1 e_a$

<https://doi.org/10.1371/journal.pone.0204755.t006>

3.3.6. Double different causes pathway (P5b). The causal equations for this model would be

$$X = input = \dot{X} + e_x$$

$$Y = input = \dot{Y} + e_y$$

$$A = m_1X + e_1 + k_1$$

$$B = m_2X + m_3Y + e_2 + k_2$$

$$C = m_3Y + e_3 + k_3$$

where e_x, e_y, e_1, e_2, e_3 are not correlated. Regression parameters derived are in [Table 7](#).

Two specific predictions of this pathway shared only by the convergent pathway (P3) are that $r_{AC}^2 = 0$ and that $r_{AB}^2 + r_{BC}^2 < 1$.

Prediction R1: $r_{AC}^2 - r_{AB}^2 r_{BC}^2 < 0$

Prediction R2: $|M_{ca}| < M_{cb} M_{ba}$

Prediction R3: The correlation $r_{E_{ba}E_{cb}}$ is predicted to have the same sign as M_{cb} .

Prediction R4: (a) $r_{BC} > r_{E_{ba}C}$ and further (b) $\frac{|r_{BC}^2 - r_{E_{ba}C}^2|}{\max(r_{BC}^2, r_{E_{ba}C}^2)} = r_{AB}^2$ is true.

It can be seen that all predictions of pathways P5a and P5b are identical and henceforth we will treat both of them in a single group as pathway P5.

3.3.7. Positive or negative feedback pathway (P6). The causal equations for this model would be

$$A = input$$

$$\frac{dB}{dt} = m_1A - d_1B + e_1 + m_fC + k_1$$

$$\frac{dC}{dt} = m_2B - d_2C + e_2 + k_2$$

where e_a, e_1, e_2 are not correlated, and d_1 and d_2 are positive. For a consistent definition of feedback, we assume m_1 and m_2 to always be positive, and that the sign of m_f decides whether it is a positive or negative feedback loop. Feedback loops depend crucially on the relative strength of the forward versus backward causation. If the feedback term, i.e. the effect of C on B is weak, it approximates to a linear pathway, and if the forward term i.e. effect of B on C is weak, it approximates to a convergent pathway. Therefore, the predictions of linear or convergent pathways can be expected if the forward or feedback links respectively are weak. Additionally, however, the negative feedback pathway is associated with a problem of definition. If the feedback effect of C on B is stronger than the effect of B on C , the signs of the slope in the causal

Table 7. Relationship between the causal and regression equations for double different cause pathway.

Slopes	Errors
$M_{ba} = \frac{m_2}{m_1} r_{AX}^2$	$E_{ba} = m_2 e_x (1 - r_{AX}^2) + m_3 e_y + e_2 - \frac{m_2}{m_1} r_{AX}^2 e_1$
$M_{cb} = \frac{m_4}{m_3} r_{BY}^2$	$E_{cb} = m_4 e_y (1 - r_{BY}^2) + e_3 - \frac{m_4}{m_3} r_{BY}^2 (m_2 e_x + e_2)$
$M_{ca} = 0$	$E_{ca} = m_4 e_y + e_3$

<https://doi.org/10.1371/journal.pone.0204755.t007>

and regression equations could be opposite, implying that while m_2 is positive, M_{cb} could become negative. This happens when

$$M_{cb} = \frac{m_2}{d_2} + \frac{\sum e_1 e_2}{\sum e_b^2} < 0 \text{ i.e. } \left| m_f \frac{\sum e_2^2}{\sum e_b^2} \frac{1}{(d_1 d_2 - m_2 m_f)} \right| > \frac{m_2}{d_2}$$

This results in a paradoxical transformation of a causally negative feedback into an apparent positive feedback since the sign of the slope and that of the feedback effect is the same. Further, when the negative feedback is much stronger than the forward effect, the predictions of convergent pathway are more applicable than the predictions of negative feedback pathway. At equilibrium where both $\frac{dB}{dt}$ and $\frac{dC}{dt} = 0$, the equilibrium concentrations of B and C are given by

$$B = \frac{m_1 d_2}{(d_1 d_2 - m_2 m_f)} A + \frac{d_2 e_1 + m_f e_2}{d_1 d_2 - m_2 m_f} + \frac{m_f k_2 + k_1 d_2}{d_1 d_2 - m_2 m_f}$$

$$C = \frac{m_2}{d_2} B + \frac{e_2}{d_2} + \frac{k_2}{d_2}$$

For simplification we take $m'_1 = \frac{m_1 d_2}{(d_1 d_2 - m_2 m_f)}$, $e'_1 = \frac{d_2 e_1 + m_f e_2}{d_1 d_2 - m_2 m_f}$ and $k'_1 = \frac{m_f k_2 + k_1 d_2}{d_1 d_2 - m_2 m_f}$

$$B = m'_1 A + e'_1 + k'_1$$

Similarly, $m'_2 = \frac{m_2}{d_2}$, $e'_2 = \frac{e_2}{d_2}$ and $k'_2 = \frac{k_2}{d_2}$

$$C = m'_2 B + e'_2 + k'_2$$

It should be noted that $e'_1 = \frac{d_2 e_1 + m_f e_2}{d_1 d_2 - m_2 m_f}$ and $e'_2 = \frac{e_2}{d_2}$ share e_2 , and would therefore co-vary. The sign of this covariance is decided by the sign of m_f , i.e. whether the feedback is positive or negative.

Regression parameters can be derived from the above as in [Table 8](#).

Prediction R1: When the feedback is negative $r_{AC}^2 > r_{AB}^2 r_{BC}^2$

The reverse applies for positive feedbacks where $r_{AC}^2 < r_{AB}^2 r_{BC}^2$

Prediction R2: In negative feedback $M_{ca} > M_{cb} M_{ba}$ and in positive feedback $|M_{ca}| < M_{cb} M_{ba}$.

Prediction R3: The sign of this correlation will be decided by the sign of m_f which is negative for negative feedback and positive for positive feedback.

Prediction R4: (a) It can be shown that for negative feedbacks $r_{E_{ba}C} < (r_{BC})$. For positive feedback the prediction is more conditional. The inequality $r_{E_{ba}C} < (r_{BC})$ will be true above a threshold r_{BC} . For smaller r_{BC} it is difficult to make a definite prediction. (b) for negative feedback $\frac{r_{BC}^2 - r_{E_{ba}C}^2}{r_{BC}^2} > r_{AB}^2$ and for positive feedback $\frac{r_{BC}^2 - r_{E_{ba}C}^2}{r_{BC}^2} < r_{AB}^2$ is true above a threshold r_{BC} .

Table 8. Relationship between the causal and regression equations for positive or negative feedback pathway.

Slopes	Errors
$M_{ba} = m_1 = \frac{m_1 d_2}{(d_1 d_2 - m_2 m_f)}$	$E_{ba} = e_1 = \frac{d_2 e_1 + m_f e_2}{d_1 d_2 - m_2 m_f}$
$M_{cb} = m_2 + \frac{\sum e_1 e_2}{\sum e_b^2} = \frac{m_2}{d_2} + \frac{\sum e_1 e_2}{\sum e_b^2}$	$E_{cb} = e_2 - \frac{\sum e_1 e_2}{\sum e_b^2} e_b = \frac{e_2}{d_2} - \frac{\text{cov}\left(\frac{d_2 e_1 + m_f e_2}{d_1 d_2 - m_2 m_f}, \frac{e_2}{d_2}\right)}{\sum e_b^2} e_b$
$M_{ca} = m_2 m_1 = \frac{m_2}{d_2} \frac{m_1 d_2}{(d_1 d_2 - m_2 m_f)}$	$E_{ca} = m_2 e_1 + e_2 = \frac{m_2}{d_2} \frac{d_2 e_1 + m_f e_2}{d_1 d_2 - m_2 m_f} + \frac{e_2}{d_2}$

<https://doi.org/10.1371/journal.pone.0204755.t008>

3.3.8. Positive or negative feed-forward pathway (P7). The causal equations for this model would be

$$A = input = \dot{A} + e_a$$

$$A = m_1X + e_1 + k_1$$

$$\frac{dB}{dt} = m_1A - d_1B + e_1 + k_1$$

$$\frac{dC}{dt} = m_2B + m_3A - d_2C + e_2 + k_2$$

where e_a, e_1, e_2 are not correlated. At equilibrium

$$B = \frac{m_1}{d_1} A + \frac{e_1}{d_1} + \frac{k_1}{d_1} = m_1A + e_1 + k_1 \text{ taking } m_1 = \frac{m_1}{d_1}, e_1 = \frac{e_1}{d_1} \text{ and } k_1 = \frac{k_1}{d_1}$$

$$C = \frac{m_1m_2 + d_1m_f}{d_1d_2} A + \left(\frac{m_2}{d_1d_2} e_1 + \frac{1}{d_2} e_2 \right)$$

$$C = \frac{m_1m_2 + m_f d_1}{d_2m_1} B - \frac{m_f}{m_1d_2} e_1 + \frac{e_2}{d_2} + \frac{k_2}{d_2}$$

$$\text{We will take } m_2 = \frac{m_1m_2 + m_f d_1}{d_2m_1} e_2 = \frac{-m_f}{m_1d_2} e_1 + \frac{e_2}{d_2}$$

Note that since e_1 decides both e_1 and e_2 , the covariance between e_1 and e_2 will be $\frac{-m_f}{m_1d_2} e_1$, which will be positive when m_f is negative i.e. for negative feed-forward, and negative when m_f positive i.e. positive feed-forward is.

For simplifying the definition of feed-forward, we assume m_1 and m_2 to be positive and the sign of m_f decides whether the feed-forward is positive or negative; a negative feed-forward pathway is once again associated with a problem of definition. If the feed-forward effect of A on C is stronger than that through B , and if their signs are opposite, the signs of slope in the causal and regression equations could be opposites. That is, if $m_f d_1 > m_1 m_2$ then M_{cb} can be negative although the causal relationship between B and C is positive. This results in a paradoxical transformation of a causally negative feed-forward pathway into an effectively positive feed-forward pathway as the product $M_{ba}M_{cb}$ and M_{ca} both have the same sign.

Note that while all the expressions are the same as in feedback pathways (Table 9), the differences lie in the meanings of $\sum e'_1 e'_2, m'_2$ etc.

Prediction R1: For positive feed-forward $r_{AC}^2 > r_{AB}^2 r_{BC}^2$, and for negative feed-forward $r_{AC}^2 < r_{AB}^2 r_{BC}^2$, but under conditions in which the result mimics positive feedback, $r_{AC}^2 > r_{AB}^2 r_{BC}^2$. This is the condition when a causally negative feed-forward transforms into an apparent positive feed-forward.

Table 9. Relationship between the causal and regression equations for positive or negative feed-forward pathway.

Slopes	Errors
$M_{ba} = m_1 = \frac{m_1}{d_1}$	$E_{ba} = e_1 = \frac{e_1}{d_1}$
$M_{cb} = m_2 + \sum \frac{e_1 e_2}{e_b^2} = \frac{m_1 m_2 + m_f d_1}{d_2 m_1} + \sum \frac{e_1 e_2}{e_b^2}$	$E_{cb} = e_2 - \sum \frac{e_1 e_2}{e_b^2} e_b = \frac{-m_f}{m_1 d_2} e_1 + \frac{e_2}{d_2} - \sum \frac{e_1 e_2}{e_b^2} e_b$
$M_{ca} = m_2 m_1 = \frac{m_1 m_2 + m_f d_1}{d_2 m_1} \cdot \frac{m_1}{d_1}$	$E_{ca} = m_2 e_1 + e_2 = \frac{m_1 m_2 + m_f d_1}{d_2 m_1} \cdot \frac{e_1}{d_1} + \frac{-m_f}{m_1 d_2} e_1 + \frac{e_2}{d_2}$

<https://doi.org/10.1371/journal.pone.0204755.t009>

Prediction R2: When m_f is positive, $M_{cb}M_{ba} < M_{ca}$. In the case of negative feed-forward $M_{cb}M_{ba} > M_{ca}$ but under conditions in which a negative feed-forward transforms into a positive feed-forward, $M_{cb}M_{ba} < m_1m_2 = M_{ca}$.

Prediction R3: For positive feed-forward, we expect a negative correlation, and for negative feed-forward, a positive correlation. Therefore, for positive feed-forward, the correlation $r_{E_{ba}E_{cb}}$ will have the opposite sign of that of M_{cb} . For a negative feed-forward pathway, under conditions when it transforms into an effective positive feed-forward correlation, $r_{E_{ba}E_{cb}}$ will have the opposite sign of that of M_{cb} .

Prediction R4: (a) In the case of positive feed-forward $r_{E_{ba}C} < r_{BC}$ and in the case of negative feed-forward prediction is conditional. Under the conditions when a causally negative feed-forward becomes apparently positive feed-forward, the prediction of positive feed-forward is true. When a negative feed-forward is effective $r_{E_{ba}C} < r_{BC}$ will be true above a threshold r_{AB} .

(b) For positive feed-forward $\frac{r_{BC}^2 - r_{E_{ba}C}^2}{r_{BC}^2} > r_{AB}^2$. For negative feed-forward a universal prediction cannot be made. When the effect is that of a positive feedback the prediction of positive feedback is true, otherwise $\frac{r_{BC}^2 - r_{E_{ba}C}^2}{r_{BC}^2} < r_{AB}^2$.

4. Testing against the null hypotheses

Testing in data needs to be different for equality and inequality predictions. The prediction can serve as the null model wherever equality is predicted but needs to be treated as an alternative hypothesis wherever inequality is predicted. For pathways that predict equality, a two-tailed probability is used, and for pathways predicting one-way inequality, a one-tailed test is used. Numerical simulations were run using the causal pathway equations for each of the pathways P1 to P7 to generate data, assuming the errors to be distributed normally around a mean zero. In the results of simulations reported below, the convention consistently followed through Figs 2 and 3 is that if H_0 is true, it is indicated by green, while H_1 being true is indicated by red and H_2 being true by yellow.

R1: $H_0: r_{AC}^2 = r_{AB}^2 r_{BC}^2$, $H_1: r_{AC}^2 < r_{AB}^2 r_{BC}^2$ and $H_2: r_{AC}^2 > r_{AB}^2 r_{BC}^2$. Since every correlation coefficient is associated with a confidence interval, to test the null hypothesis, we check that the confidence interval of $r_{AC}^2 - r_{AB}^2 r_{BC}^2$ includes zero.

R2: $H_0: M_{ca} = M_{cb}M_{ba}$ (green), $H_1: M_{ca} < M_{cb}M_{ba}$ (red) and $H_2: M_{ca} > M_{cb}M_{ba}$ (yellow).

R3: Since the signs of causal slopes m_1 and m_2 are allowed to be positive or negative in the models, the correlation coefficients are multiplied by the sign of the slope M_{cb} .

Rule	Linear	Radiating	Converging	Common Cause	Different Cause	Feedback		Feedforward	
						-	+	-	+
R1	Green	Green	Red	Yellow	Red	Red	Red	Yellow	
R2	Green	Green	Red	Yellow	Red	Red	Red	Yellow	
R3	Green	Green	Yellow	Red	Yellow	Yellow	Red	Red	
R4a	Red	Red	Yellow	Red	Yellow	Red	Red*	Red**	Red
R4b	Green	Green	Green	Yellow	Green	Yellow	Red	Red	Yellow

Fig 2. Analytical signatures for each pathway. Summarizing the analytical signature for each pathway in a color code where green represents acceptance of the null hypotheses H_0 , and red and yellow represent the acceptance of H_1 and H_2 respectively. Asterisks indicate conditional prediction e.g. r_{BC}^2 above a threshold, r_{AB}^2 above a threshold.

<https://doi.org/10.1371/journal.pone.0204755.g002>

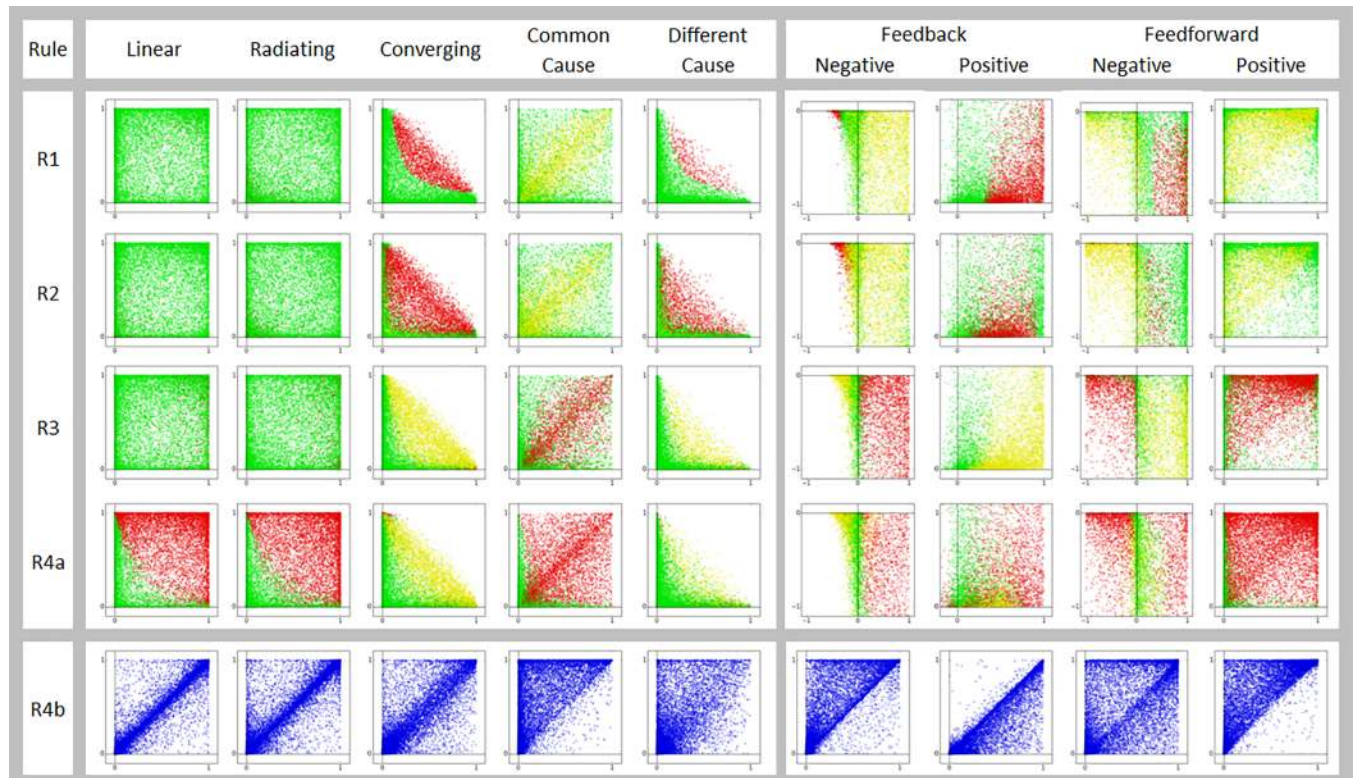


Fig 3. Simulation results of all pathways against all predictions. For all acyclic pathways and predictions from R1 to R4a, the result of every simulation run is plotted as a point with r_{AB}^2 and r_{BC}^2 on X and Y axes respectively. Green represents null hypothesis true, red for H_1 and yellow for H_2 .

<https://doi.org/10.1371/journal.pone.0204755.g003>

$H_0: r_{E_{ba}E_{cb}}^2 \cdot \text{sign}(M_{cb}) = 0$ (green), $H_1: r_{E_{ba}E_{cb}}^2 \cdot \text{sign}(M_{cb}) < 0$ (red) and $H_2: r_{E_{ba}E_{cb}}^2 \cdot \text{sign}(M_{cb}) > 0$ (yellow).

R4a: $H_0: r_{BC}^2 = r_{E_{ba}C}^2$ (green), $H_1: r_{BC}^2 < r_{E_{ba}C}^2$ (red) and $H_2: r_{BC}^2 > r_{E_{ba}C}^2$ (yellow).

R4b: $H_0: \frac{|r_{BC}^2 - r_{E_{ba}C}^2|}{\max(r_{BC}^2, r_{E_{ba}C}^2)} = r_{AB}^2$, $H_1: \frac{|r_{BC}^2 - r_{E_{ba}C}^2|}{\max(r_{BC}^2, r_{E_{ba}C}^2)} < r_{AB}^2$, $H_2: \frac{|r_{BC}^2 - r_{E_{ba}C}^2|}{\max(r_{BC}^2, r_{E_{ba}C}^2)} > r_{AB}^2$. Since the prediction is

about whether $\frac{|r_{BC}^2 - r_{E_{ba}C}^2|}{\max(r_{BC}^2, r_{E_{ba}C}^2)}$ is predicted by r_{AB}^2 , in the simulations results reported below we

show a scatter plot between the two where good predictions lie along the diagonal and failure of prediction strays away from it.

The results match very well with the predictions in Fig 2. For converging and different cause pathways, a pathway specific prediction is that the sum of the two correlation coefficients never exceeds unity. This is also evident in the simulation results.

For feedback and feed-forward pathways predictions from R1 to R4a, the X axis is r_{BC} and Y is $\frac{m_2 s d e_1}{m_f s d e_2}$ which reflects the relative strength of the feedback or feed-forward term as compared to the forward relation between B and C. The feed effect is strong when the ratio is close to zero and weak moving away from it. For negative feedback and feed-forward the Y axis goes from -1 to 0 and for positive feedback and feed-forward from 0 to 1. With negative feedback and feed-forward, there is an apparent conversion to positive feedback and feed-forward respectively under a set of conditions. When this happens r_{BC} becomes negative and the predictions of positive feedback and feed-forward respectively apply. It can also be seen that when the ratio is close to zero, predictions of converging pathway hold true.

Predictions from R4b for all pathways are shown as scatter plots with $\frac{|r_{BC}^2 - r_{EbaC}^2|}{\max(r_{BC}^2, r_{EbaC}^2)}$ and r_{AB}^2

When they are predicted equal, most points lie along the diagonal. Wherever inequality is predicted, they are on one side of the diagonal.

Rejection due to overfitting inequality: For all inequality predictions, overfitting is possible. For example, if we expect that $r_{AC}^2 > r_{AB}^2 r_{BC}^2$, it is also possible that r_{AC}^2 is too large than what can be predicted by the pathway under consideration. It is possible to test this either analytically using equations derived for the corresponding predictions (see [S1 Text](#)), or using simulations only if the parameters of the causal equations are known. If parameter estimates for the pathways are known from independent empirical sources, it should be possible to test over-fitting inequality. We will illustrate this with real life data later in the section ‘Testing specific pathways and questions: The case of pre-diabetes’.

5. Sensitivity and robustness of predictions

We used simulations to test the sensitivity and reliability of the analytical predictions. The simulations were run using the causal pathway equations for each of the pathways P1 to P7 to generate data, assuming the errors to be distributed normally around a mean zero. Up to 10000 simulations are run, with each run using randomly drawn parameters and error standard deviations from a given range (see [S1 Text](#) ‘Simulations used for testing the sensitivity and robustness of the predictions’ for details). The error standard deviation ranges were selected such that the coefficients of determination were well spread between zero and one. The generated data were then used to test the predictions of the corresponding pathway. Simulations used in this section are not based on real life data and are mainly employed to test the reliability of the predictions over a range of regression correlation coefficients.

5.1. Prediction sensitivity depends on sample size

Figs 2 and 3 show that simulations generally follow the analytical predictions quite well, but with certain limitations. Many of the predictions, particularly when H_1 and H_2 are expected to be true, work well above threshold values of r^2 . When either r_{AB}^2 or r_{BC}^2 or both are small, the null hypothesis fails to get rejected. This threshold of sensitivity can be reduced by increasing sample size (n) ([Fig 4](#)). For example, in the case of prediction 1 for the convergent pathway, simulations showed that type 2 error reduced in a threshold relationship with the product of r_{AB}^2 and r_{BC}^2 and the point of inflection reduced exponentially with sample size ([Fig 4B](#)). Although qualitatively it can be said without doubt that statistical power would increase with sample size, the effect of sample size on statistical power appears to be different for different pathway-prediction combinations ([Fig 4](#)). In the case of cyclic pathways, many predictions are conditional as described above, and that is clearly reflected in the simulations. The agreement between predictions and simulation results is weaker for a few specific pathway-prediction combinations, in the sense that they work in a narrow range of conditions. This was seen in case of P5 (different cause) prediction from R4b, and P7 (negative feed-forward) prediction from R2 ([Fig 4](#)). This implies that we need to be conservative in rejecting pathways in such pathway-prediction combinations, particularly when the correlation coefficients are small. Further, wherever the predictions are themselves the null models, its rejection will naturally become conservative at low correlations. However, for inequality predictions, where the null hypothesis is equality, failure of rejecting the null hypothesis should not be taken as rejection of the prediction when correlations are weak. When we take such a conservative approach, rejection of a prediction can be confidently taken to mean rejection of a pathway whereas failure to reject has limited implications particularly when the correlations are weaker.

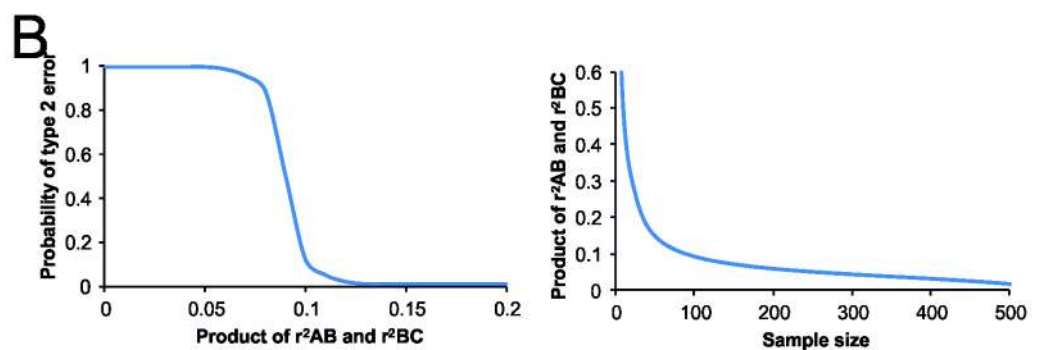
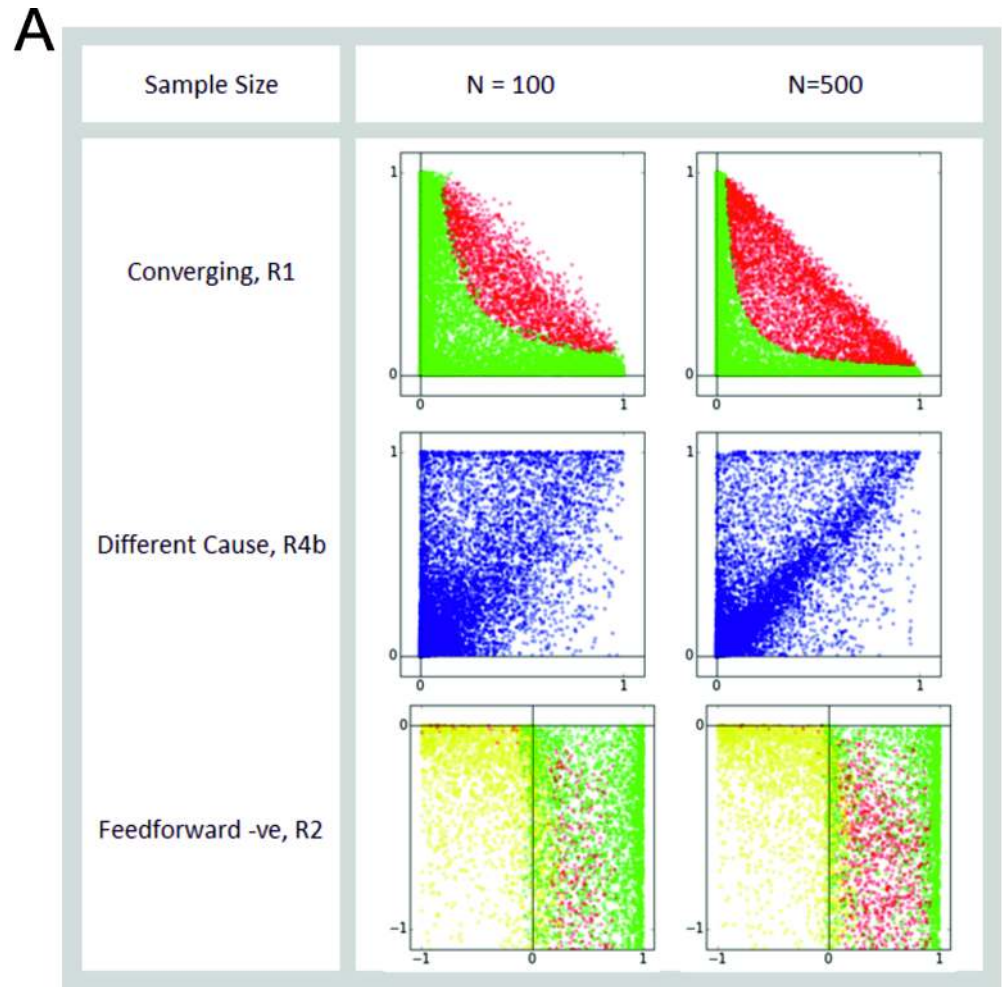


Fig 4. Effect of n on the reliability of prediction. **A:** Simulation results at $n=100$ and $n=500$ in three pathway-prediction combinations: Colour codes similar to Fig 3. Note that when correlation coefficients are small the null hypothesis fails to get rejected leading to type 2 error. The parameter area over which the simulation results match the prediction increases with n . **B:** For prediction 1 of convergent pathway type 2 error shows a threshold relationship with the product of r_{AB}^2 or r_{BC}^2 and the point of inflection of the threshold relationship decreases exponentially with sample size.

<https://doi.org/10.1371/journal.pone.0204755.g004>

5.2. Robustness of predictions

It can be seen from Table 10 that each pathway makes a set of predictions by which some pathways can be differentiated from others. However, some have an identical set of predictions among

Table 10. Summary of predictions of all pathways considered.

Prediction/ Rule → Pathway ↓	R1	R2	R3	R4 a	R4 b	Pathway specific prediction
P1 linear	$r^2_{AC} - r^2_{AB} \cdot r^2_{BC} = 0$	$ M_{ca} = M_{ba} \cdot M_{cb} $	$r_{Eba,Ecb} = 0$	$r_{Ebc,C} / r_{BC} < 1$	$\frac{ r^2_{Eba,C} - r^2_{BC} }{\max(r^2_{Eba,C}, r^2_{BC})} = r^2_{AB}$	
P2 radiating	$r^2_{AC} - r^2_{AB} \cdot r^2_{BC} = 0$	$ M_{ca} = M_{ba} \cdot M_{cb} $	$r_{Eba,Ecb} = 0$	$r_{Ebc,C} / r_{BC} < 1$	$\frac{ r^2_{Eba,C} - r^2_{BC} }{\max(r^2_{Eba,C}, r^2_{BC})} = r^2_{AB}$	
P3 convergent	$r^2_{AC} - r^2_{AB} \cdot r^2_{BC} < 0$	$ M_{ca} < M_{ba} \cdot M_{cb} $	$r_{Eba,Ecb} > 0$	$r_{Ebc,C} / r_{BC} > 1$	$\frac{ r^2_{Eba,C} - r^2_{BC} }{\max(r^2_{Eba,C}, r^2_{BC})} = r^2_{AB}$	$r_{AC} = 0,$ $r^2_{AB} + r^2_{BC} < 1$
P4 common cause	$r^2_{AC} - r^2_{AB} \cdot r^2_{BC} > 0$	$ M_{ca} > M_{ba} \cdot M_{cb} $	$r_{Eba,Ecb} < 0$	$r_{Ebc,C} / r_{BC} < 1$	$\frac{ r^2_{Eba,C} - r^2_{BC} }{\max(r^2_{Eba,C}, r^2_{BC})} > r^2_{AB}$	Symmetry around A,B,C
P5 different cause	$r^2_{AC} - r^2_{AB} \cdot r^2_{BC} < 0$	$ M_{ca} < M_{ba} \cdot M_{cb} $	$r_{Eba,Ecb} > 0$	$r_{Ebc,C} / r_{BC} > 1$	$\frac{ r^2_{Eba,C} - r^2_{BC} }{\max(r^2_{Eba,C}, r^2_{BC})} = r^2_{AB}$	$r_{AC} = 0$ $r^2_{AB} + r^2_{BC} < 1$
P6 feedback Negative	$r^2_{AC} - r^2_{AB} \cdot r^2_{BC} > 0$	$ M_{ca} > M_{ba} \cdot M_{cb} $	$r_{Eba,Ecb} < 0$	$r_{Ebc,C} / r_{BC} < 1$	$\frac{ r^2_{Eba,C} - r^2_{BC} }{\max(r^2_{Eba,C}, r^2_{BC})} > r^2_{AB}$	
P6 feedback positive	$r^2_{AC} - r^2_{AB} \cdot r^2_{BC} < 0$	$ M_{ca} < M_{ba} \cdot M_{cb} $	$r_{Eba,Ecb} > 0$	$r_{Ebc,C} / r_{BC} < 1$	$\frac{ r^2_{Eba,C} - r^2_{BC} }{\max(r^2_{Eba,C}, r^2_{BC})} > r^2_{AB}$	
P7 feed-forward negative	$r^2_{AC} - r^2_{AB} \cdot r^2_{BC} < 0$	$ M_{ca} < M_{ba} \cdot M_{cb} $	$r_{Eba,Ecb} > 0$	$r_{Ebc,C} / r_{BC} < 1$	$\frac{ r^2_{Eba,C} - r^2_{BC} }{\max(r^2_{Eba,C}, r^2_{BC})} < r^2_{AB}$	
P7 feed-forward positive	$r^2_{AC} - r^2_{AB} \cdot r^2_{BC} > 0$	$ M_{ca} > M_{ba} \cdot M_{cb} $	$r_{Eba,Ecb} < 0$	$r_{Ebc,C} / r_{BC} < 1$	$\frac{ r^2_{Eba,C} - r^2_{BC} }{\max(r^2_{Eba,C}, r^2_{BC})} > r^2_{AB}$	

Note that there are 6 distinct signatures among 9 pathways. Pathways with identical predictions are shaded with the same color. There is some redundancy between the predictions. For example, the results of R1, R2 and R3 are tightly correlated. We feel that the redundancy serves to validate and reinforce the predictions. Also, when there are complex pathways arising through combinations of primary pathways, different predictions show differential departures from the primary pathway predictions. Therefore, all predictions are useful in spite of some redundancy.

<https://doi.org/10.1371/journal.pone.0204755.t010>

the general predictions described so far. Table 10 shows that there are 6 different signatures among 9 primary pathways. Some of the predictions are conditional, and therefore, it may not always be possible to differentiate between pathways. For example, some predictions do not work for very small r^2 values. Feedback is not distinguishable from linear pathways unless the feedback arrow is sufficiently strong. Such limitations are common to all statistical tools, and they need to be used and interpreted in light of the appropriate context and conditions.

5.3. Sensitivity analysis

The predictions derived and tabulated above are based on the typical assumptions of main-stream statistics that the input variables are distributed normally and that all causal links are linear. However, it is important to ask how critical these assumptions are for the predictions to work. In experimental biology, the input variable is often designed to have uniform intervals and is not normally distributed. A moderate deviation from linearity is also common in physiological and other biological systems. If the predictions are too sensitive to these assumptions, they may prove to be of limited use in real-life. We used Monte-Carlo simulations to assess whether the predictions work under moderate deviations from these assumptions. When the input variables were selected randomly from a uniform rather than a Gaussian distribution, all predictions worked with nearly the same differentiating ability (data not shown). Similarly, when non-parametric Spearman ranked correlations were used instead of Pearson's correlations, the correlation related predictions (from R1 and R4) worked similarly (data not shown). This demonstrates that the tools are not too sensitive to the assumptions of normality of input variable, linearity of relationships, and parametric or non-parametric nature of correlations.

6. Applications of the method

6.1. Accepting or rejecting pathways using real-life data

Two approaches are possible by which the predictions of a pathway can be tested using real-life data.

(i) Based on confidence intervals of correlations and regression slopes: The null hypotheses for every prediction can be tested using calculation of confidence intervals of regression correlation parameters. Simulations have shown that except when the underlying correlation coefficients are too low, this approach can be reliably used to test the predictions. The sensitivity of predictions depends upon the sample size as well as the position in the parameter space (Fig 3). It is likely therefore that at smaller sample sizes, or at lower r_{AB}^2 or r_{BC}^2 , pathways that predict H_1 or H_2 may fail to get support even if true. On the other hand, at lower r_{AB}^2 or r_{BC}^2 if a pathway predicts H_0 to be true and the null hypothesis gets rejected, the rejection can be highly reliable. **(ii) Monte-Carlo simulation approach:** An alternative approach, which will be more conservative in rejecting pathways, is the Monte-Carlo approach. Assuming a specific pathway to be true, it is possible to back calculate the causal equation parameters from the regression correlation parameters obtained in the data (Tables 2 to 9). For pathways such as negative or positive feedback, it is not possible to estimate all causal parameters from regression parameters. In such cases, if empirical estimates of one or a few causal parameters can be obtained, the remaining causal parameters can be worked back. Using the estimated parameters of causal equations, Monte-Carlo simulations can be run to obtain the probabilities of getting the observed results. This approach can be particularly useful when the correlations obtained in the data are weak, and a conservative inference is preferred.

6.2. Distinguishing between pathways with identical signatures

From the predictions summarized in Table 10, it can be seen that some pathways share prediction signatures. For example, the linear pathway cannot be distinguished from radiating or convergent, is indistinguishable from different cause. There are three possible ways of resolving between pathways with similar signatures:

- i. **Swapping variables:** In the generalized predictions, common cause pathway and negative feedback pathway have the same predictions. However, the predictions of the common cause pathway are symmetric around A, B and C, and flipping the positions of the three variables does not alter the predictions, which is not the case with negative feedback pathway.
- ii. Involving a fourth variable whose causal relationship with at least one of the triad is already known, or
- iii. Involving more variables to cross validate pathways.

We will discuss (ii) and (iii) in a different context below.

6.3. Inferring causality between two variables

It is extremely difficult to infer causal relationship between two correlated variables. Although some solutions have been suggested, their applicability is limited [15, 16]. However, it is possible to infer the causal relationship between two variables if we have data on a third variable that is correlated with one or both of them with known causality. For example, in men, testosterone levels and muscle strength are correlated, but the direction of the causal arrow might be uncertain since testosterone can increase muscle mass, while [32] exercise can also induce a testosterone response [33,34]. The causal relationship can be revealed in cross-sectional data if

we use chronological age as a third variable. Neither testosterone nor muscle mass decides the chronological age, but age may affect one or both the variables. If age shows significant correlation with one or both the variables, the predictions from different possible pathways can be tested using the set of predictions as described. By testing these predictions, it should be possible to determine the causal relationship between muscle mass and testosterone.

6.4. Inferring causal pathways with three variables

To infer causal pathways within three intercorrelated variables, three alternative approaches are possible. The first approach is to test and resolve between preconceived hypothetical pathways. It is likely that prior knowledge or some insights into mechanisms allow us to start with a few plausible alternative pathways. It is possible to perceive more complex pathways by combinations of the primary pathways that we considered in this paper. For example, a pathway may contain both feedback and feed-forward elements. Such complex or combinational pathways can be used to make a set of predictions by the analytical approach described above and testing these predictions can resolve between pathways. If we do not have such preconceived pathways, it would be necessary to consider all possible combinations of pathways between the three variables and make differential predictions from each of them. In such cases, we must also consider permutations of the variables. At the end, it may not be possible to ascertain a single unique causal pathway since the prediction signatures of some of them may be identical. Nevertheless, it would still be possible to reject some pathways based on their prediction signature. In addition, if available, we can involve a fourth variable correlated to one or more of the three, if there is some pre-existing knowledge about its causal relationship.

6.5. Inferring causal networks with more than three variables

In complex systems, often there are large causal networks. In such networks, combinations of 3 membered motifs can be identified. Out of the possible pathways among three variables some can be rejected using analysis of the three variables. Bringing in a fourth one can provide additional insights which can be used for cross checking or validating our first set of inferences. In complex causal networks, there can be many such cross check and validation possibilities. For large networks algorithms requiring massive computational power may be needed that may pin down one or a few network structures from the large number of possible ones using combinations of three-member motifs and cross validation facility among the motifs.

7. Testing specific pathways and questions: The case of pre-diabetes

Apart from some common pathways described above, it is possible that real life problems have some added complications due to which, the standard solution of testing a fixed set of predictions may not be sufficient. However, one can apply similar foundational principles to handle such pathway-specific questions. We will illustrate this using a classical hypothesis that attempts to explain a human physiological state designated as an insulin resistant, hyperinsulinemic, normoglycemic, pre-diabetic state. In this state, the plasma levels of fasting insulin (FI) are raised although fasting glucose (FG) remains normal. The classical interpretation of this state (Fig 5A) is that a rise in insulin resistance, presumably as a result of obesity, is primary. Insulin resistance interferes with insulin-induced glucose uptake by muscle and other insulin-dependent tissues. The reduced uptake raises plasma glucose levels. The raised plasma glucose induces extra insulin secretion so that plasma insulin levels go up. The extra insulin compensates for insulin resistance and normalizes glucose level. As a result, the fasting steady state of an insulin-resistant individual is characterized by raised FI and normal FG. At steady state,

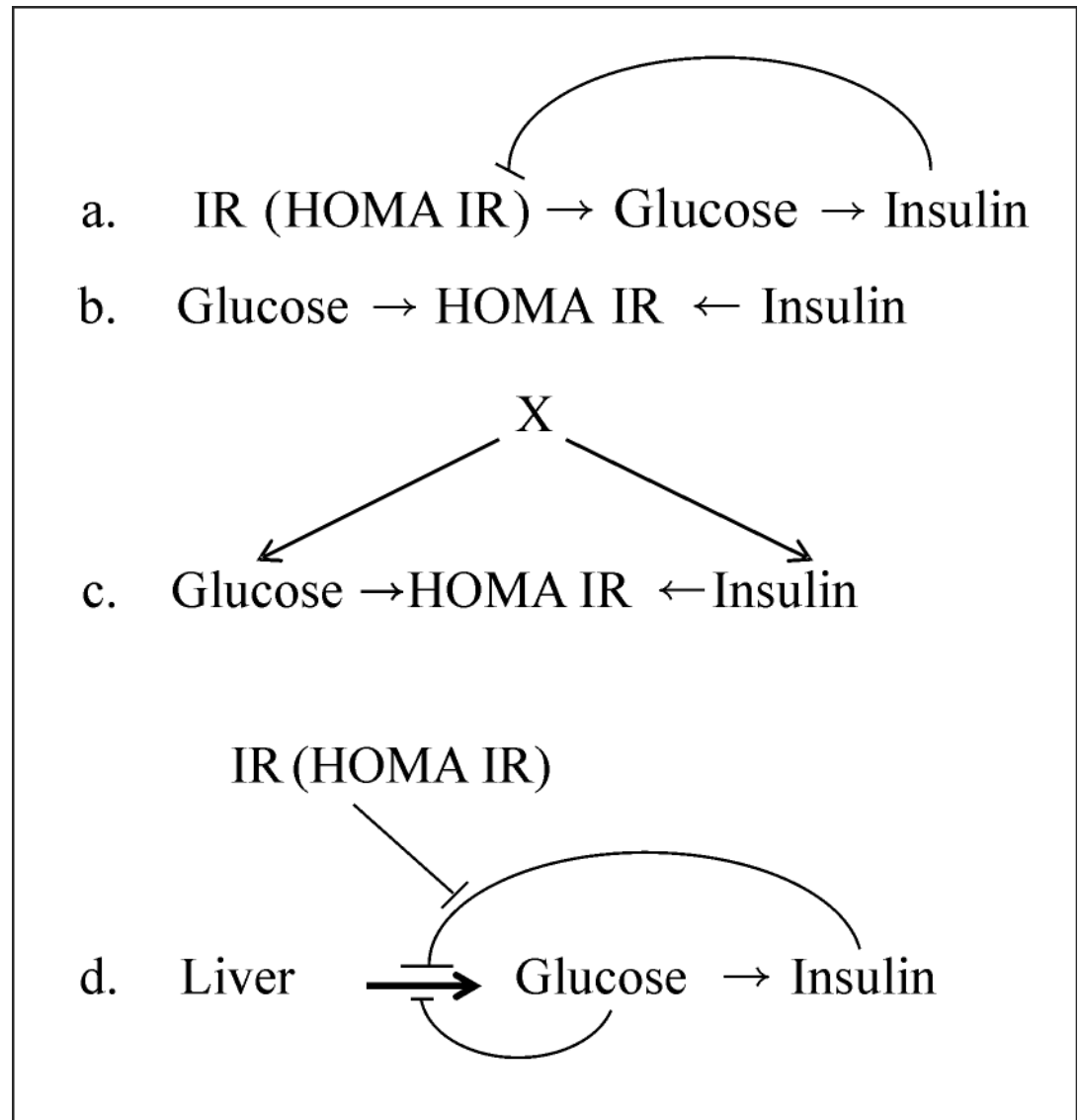


Fig 5. Possible pathways between insulin resistance, FG and FI. a) A simplified single feedback pathway that approximates the negative feedback pathway P6. b) A null model assuming FG and FI to be independent and HOMA-IR a derived construct. c) An improvised null model with an external causal factor influencing FG and FI. d) The classically perceived pathway with dual feedback from glucose and insulin.

<https://doi.org/10.1371/journal.pone.0204755.g005>

insulin resistance is measured by the index, HOMA-IR (defined as $\frac{Insulin(IU) \cdot Glucose(\frac{mg}{dL})}{405}$), and the β cell response to glucose, by the index, HOMA β (defined as $\frac{360 \cdot Insulin(IU)}{Glucose(\frac{mg}{dL}) - 63}$). Both the indices are based on the assumption of a steady state. Indices based on ratios are tricky in that they can result into many spurious correlations. These correlations are not useful to make any functional inference about the system. However, we show below that since different causal pathways can give rise to different correlations, such correlations can be used to infer causal pathways.

A logical flaw in this interpretation is that, after the glucose levels return to normal, there is no reason why FI should remain high. Insulin has a short half-life of about 6 minutes [30,35]

and therefore a steady state level can be achieved quite fast; 12 hour fasting should be sufficient to achieve such a steady state. Therefore, a steady state in which FI is raised but FG remains normal is not well explained by the classical theory. In spite of this flaw, the main stream thinking in this field has held on to this interpretation for over four decades, and the indices HOMA-IR and HOMA- β continue to be commonly used in epidemiological research. Challenges to this causal interpretation come from the arguments and evidence that rise in FI precedes insulin resistance [22–26,36]. Therefore, there is a need to reexamine the classical causal pathway. We will test this pathway based on our interpretations of the interrelationships of the regression-correlation parameters.

The pathway in question is more complex than the basic set of pathways P1 to P7. For regulation of glucose production by the liver and glucose uptake by tissues, there is a dual negative feedback. One feedback is exerted by glucose itself, which enhances tissue uptake and suppresses liver glucose production. The other feedback operates through insulin, which facilitates glucose uptake by insulin-dependent tissues and suppresses liver glucose production. If we ignore the direct glucose feedback and assume that feedback regulation operates only through insulin, then there is a single negative feedback. Thus the pathway can be simplified to the negative feedback pathway P6. If we incorporate dual feedback, as the equations show below, the relationship between insulin resistance and FG is not strictly linear. We could therefore use the standard set of predictions of a negative feedback model, assuming a single feedback. Alternatively, we can use the dual feedback model, and apply simulations to make and test predictions, since empirical estimates for most of the parameters are available from experiments (see [S2 Text](#)).

However, the main problem in testing these pathways is that we have no direct measure of insulin resistance. HOMA-IR and HOMA- β are believed to measure insulin resistance and β cell response respectively, but they are derived from the other two variables, which makes the problem tricky and circular. We approach the problem using more than one set of assumptions. (i) First, we test the dual feedback pathway ([Fig 5D](#)) assuming HOMA-IR and HOMA- β to faithfully represent insulin resistance and β cell response respectively. (ii) Then, we examine the constraints laid down by deriving these two parameters from the other two variables. (iii) In comparison, we use a null model ([Fig 5B](#)) in which the classical pathway is not true, there is no relationship between FG and FI, and HOMA-IR and HOMA- β are artificial constructs derived from the two measured variables and may not reflect any real phenomenon. We also test the typical convergent model, in which FG and FI determine HOMA-IR. (iv) Using some oversimplification, ignoring non-linearity of the model and assuming that HOMA-IR and HOMA- β are faithful indicators, we test the classical predictions of the negative feedback pathway ([Fig 5A](#)) as described earlier. We use epidemiological data on FG and FI measurements in four populations to test the classical causal pathway using our approach.

As a general note, we would like to add that the HOMA indices being ratio measures could be confounding factor. It is known that ratio indices can behave unpredictably in different parameter ranges, and can therefore generate spurious correlations. In our view, this strengthens the case for using the underlying causal relationships between the variables to interpret these correlations in the appropriate context.

7.1. Data sources

We used four data sets of sample studies by two research groups. All the four sets contain individuals with and without overt type 2 diabetes. Since we are addressing the prediabetic state here we have taken the non-diabetic subset of n individuals from the four samples. (i) Coronary Risk of Insulin Sensitivity in Indian Subjects (CRISIS) Study, Pune, India [37] ($n=558$).

(ii) Pune Maternal Nutrition Study (PMNS), Pune, India [38] (n=299). (iii and iv) Newcastle Heart Project (NHP), England, [39] which has data on populations of two different ethnic origins namely European white (n=595) and south Asian (n=413). (iv) Pune Maternal Nutrition Study (PMNS), Pune, India [38] (n=299). We received the data from the two principal investigators of the studies. Data sources (i) and (ii) were received from Prof. Chittaranjan Yajnik and data sources (iii) and (iv) were received from Prof. Raj Bhopal. All data have been anonymized, and all the predictions have been tested independently in all the four data sets.

7.2. The dual feedback model (Fig 5D)

We assume that the standing plasma glucose level is a result of baseline rate of glucose production by the liver; suppression of this production as well as muscle glucose pickup which is proportional to the standing glucose level (direct glucose feedback); the insulin mediated suppression as well as uptake (insulin mediated feedback) and individual variability. The standing insulin levels are a result of glucose stimulated insulin secretion on the one hand and insulin degradation on the other. Thus, the causal equations can be written as

$$\frac{dG}{dt} = L - K_1 \cdot G - I_{SENS} \cdot K_2 \cdot I + e_1$$

$$\frac{dI}{dt} = K_3 \cdot G - d \cdot I + e_2$$

Where G and I are plasma levels of glucose and insulin respectively, and FG and FI are the fasting steady state levels of the same. K_1 denotes the rate constant for negative feedback of glucose on liver glucose production and tissue glucose uptake; K_2 denotes the rate constant for insulin-mediated feedback which is proportional to I_{SENS} , the insulin sensitivity of tissues; K_3 is the rate constant for glucose-induced insulin release; and d , the rate of insulin degradation.

At steady state, we get

$$FG = \frac{d \cdot (L + e_1) - I_{SENS} \cdot K_2 \cdot e_2}{K_1 \cdot d + I_{SENS} \cdot K_2 \cdot K_3}$$

$$FI = \frac{K_3 \cdot FG + e_2}{d}$$

It can be seen that the steady state glucose level is a function of insulin resistance (IR) which is a reciprocal of insulin sensitivity. Using the reciprocal, we can write

$$FG = \frac{IR \cdot d \cdot (L + e_1) - K_2 \cdot e_2}{IR \cdot K_1 \cdot d + K_2 \cdot K_3}$$

Thus the relationship between FG and IR is non-linear and follows a saturation curve.

7.3. Testing the model

Testing the pathways by the four different approaches described above:

7.3.1. Approach 1. Assuming classical pathway and faithful indices: The following predictions of the classical pathway depicted in Fig 5D and modeled above are testable.

- i. HOMA-IR, FG and FI should be positively correlated to each other. This prediction is true in all the four data sets except that the correlations between FG and FI are weak in all the four data sets. In terms of the variance explained (range 2.6 to 4.9%) FG and FI are poorly

Table 11. Fasting glucose and fasting insulin in the four datasets.

Data source	FG mean (s.d.)	FI mean (s.d.)
CRISIS (n=558)	94 (18.70)	7.58 (1.82)
KEMPMNS (n=299)	86.35 (11.21)	11.84 (10.82)
NHP-SA (n=413)	98.86 (7.37)	11.11 (9.26)
NHP-EU (n=595)	99.90 (6.40)	8.41 (5.29)

<https://doi.org/10.1371/journal.pone.0204755.t011>

related (Table 11). The glucose homeostasis model expects a positive correlation between FG and FI. It is important to realize this since in the classical thinking, a prediabetic state is characterized by increased insulin but normal glucose levels. If the compensatory insulin response is mediated through glucose, it is impossible to have a raised FI without a proportionate rise in FG. In the pathway predictions, a positive correlation between FG and FI is expected independent of the feedback loop. However the classical thinking tries to explain a hyperinsulinemic normoglycemic state achieved through this pathway. The poor correlation between FG and FI, and a large coefficient of variation in FI compared to FG indicates that a normoglycemic hyperinsulinemic state may indeed be achieved, but whether the classical pathway offers a sound explanation for this state is the question. In an insulin resistant state, the level of FI can increase by about 10-fold the normal. However, the difference between the lower and upper limit of glucose in a pre-diabetic state is less than 1.5-fold. To achieve a tenfold increase in the effect resulting from a 1.5 fold increase in the causal variable, the slope needs to be of the order of 7 to 8. However in the data, the regression slope ranges between 0.05 and 0.2 (Table 12). Therefore the variance in FI is unlikely to be caused by variance in glucose following insulin resistance. Therefore, we need to conclude that most of the variation in FI appears to be random error independent of insulin resistance.

- ii. By the steady state equations, the slope of the regression of FI on FG should be K_3/d . Empirical estimates for both K_3 and d are available (see S2 Text) and therefore this prediction can be tested. The empirical estimates are $K_3 = 0.08$ microIU.mg/min and $d = 0.15$ /min respectively, and thereby the expected slope is 0.533. In all the four data sets, the slopes are significantly smaller than the ones predicted from the empirical estimates (0.05 to 0.2). Thus, apart from a mismatch between the slope required to cause the observed variation in FI and actual slopes, the slopes expected from the empirical estimates of parameters and those obtained in regression also do not match. The latter mismatch by itself may not be sufficient to reject the pathway since a large measurement error in the X variable, i.e. FG can lead to underestimation of regression slope, but this explanation implies that a substantial part of variation in glucose is independent of insulin resistance, and is akin to random error with respect to the hypothetical causal pathway.
- iii. HOMA- β in our assumption represents K_3 . However K_3 is a constant in our model, and although it may have some variability in the population, it is uncorrelated with the three variables of concern. Therefore, HOMA- β should show no significant correlation with FG, FI and HOMA-IR. However, in all the four data sets HOMA- β is significantly positively correlated with FI, but negatively correlated with FG and positively correlated with HOMA-IR.
- iv. In a negative feedback pathway $r_{AC}^2 > r_{AB}^2 \cdot r_{BC}^2$. Qualitatively this inequality is true for HOMA-IR, FG and FI in the data. However, simulations show that there is overfitting of the inequality. r_{AC}^2 in all the four sets of data are substantially higher than the distribution obtained in the simulations (Fig 6). The correlation between FI and HOMA-IR is far greater than that predicted by the simulations, leading to an overfitting rejection.

Table 12. Correlations between FG, FI, HOMA-IR and HOMA beta in the four data sets; r is the Pearson’s correlation coefficient, M is the slope of the corresponding regression, and ρ is the Spearman’s rank correlation.

	FG:FI		FG:HOMA IR		FG:HOMA beta		FI:HOMA IR		FI:HOMA beta		HOMA IR:HOMA beta	
	r(M)	ρ	r	ρ	r	ρ	r	ρ	R	ρ	r	ρ
CRISIS (n=558)	0.217 (0.055)	0.284	0.525	0.465	-0.209	-0.403	0.931	0.975	0.232	0.698	0.312	0.543
KEM PMNS(n=299)	0.198 (0.191)	0.241	0.317	0.352	-0.219	-0.259	0.985	0.990	0.532	0.811	0.633	0.746
NHP-SA (n=413)	0.163 (0.206)	0.282	0.236	0.464	-0.198	-0.145	0.995	0.990	0.763	0.875	0.833	0.810
NHP-EU (n=595)	0.223 (0.185)	0.261	0.309	0.464	-0.064	-0.055	0.994	0.993	0.891	0.933	0.904	0.886

<https://doi.org/10.1371/journal.pone.0204755.t012>

Thus if we assume the two HOMA indices to faithfully represent insulin resistance and beta cell response respectively, then classical pathway needs to be rejected owing to mismatches with many of its predictions.

The distribution generated by simulations matches well with the real life correlations for true IR-FG (grey bars and arrows), FG-FI (red bars and arrows), and the product of the two (purple bars and arrows). The correlation between true IR and FI is greater than the product as predicted by the pathway (green bars, we do not have empirical estimates of these correlations) but the correlation between HOMA-IR and FI (blue bars and arrows) is substantially greater than the predicted leading to an overfitting rejection. This indicates that either HOMA-IR as currently calculated is substantially different from true insulin resistance or the pathway get rejected based on this prediction.

7.3.2. Approach 2. Effects of deriving HOMA-IR and HOMA-β from FG and FI: Since HOMA-IR and HOMA-β are not independently measured but derived from FG and FI measurements, some correlations will follow from the derivations themselves. The overfitting anomaly observed above can be explained as an artifact coming out of the calculation of HOMA-IR. However, some other anomalies remain unexplained. Here we are assuming that the classical pathway is true and therefore, FI is a linear function of FG. If FI is represented as $m.FG + e$, HOMA-IR will be correlated to FG^2 . Similarly, HOMA-β should be represented as $m.FG/(FG - 63)+e$. Under normal physiological range, $FG > 63$ and therefore HOMA-β is a decreasing function of FG. As a result both FI and HOMA-IR should be negatively correlated to HOMA-β. Simulations of the pathway results in a negative correlation between HOMA-IR and HOMA-β as long as the errors are small to moderate. These expectations do not match the empirical data, in which FI and HOMA-IR have significant positive correlations with HOMA-β. Thus, accepting the classical pathway with some allowance for artifacts coming out of the derived variables is not sufficient to explain the empirical correlations.

7.3.3. Approach 3. Testing the predictions of the null model: If FG and FI are independent of each other and have some variance around a mean, HOMA-IR is expected to be positively correlated with both since it is a product of the two. FI should be positively correlated with HOMA-β, but FG should be negatively correlated with HOMA-β. In the HOMA-IR-HOMA-β relationship, FI is in the numerator of both. FG is in the numerator of HOMA-IR but in the denominator of HOMA-β. Nevertheless, since the coefficient of variation of FI is substantially greater than that of FG, FI is expected to dominate the relationship and result in a positive correlation between HOMA-IR and HOMA-β. All these predictions are observed in the data (Table 12). The mismatch of the null model with the data is that it assumes FG and FI to be independent and uncorrelated. In all the four sets of data, there is a significant but weak

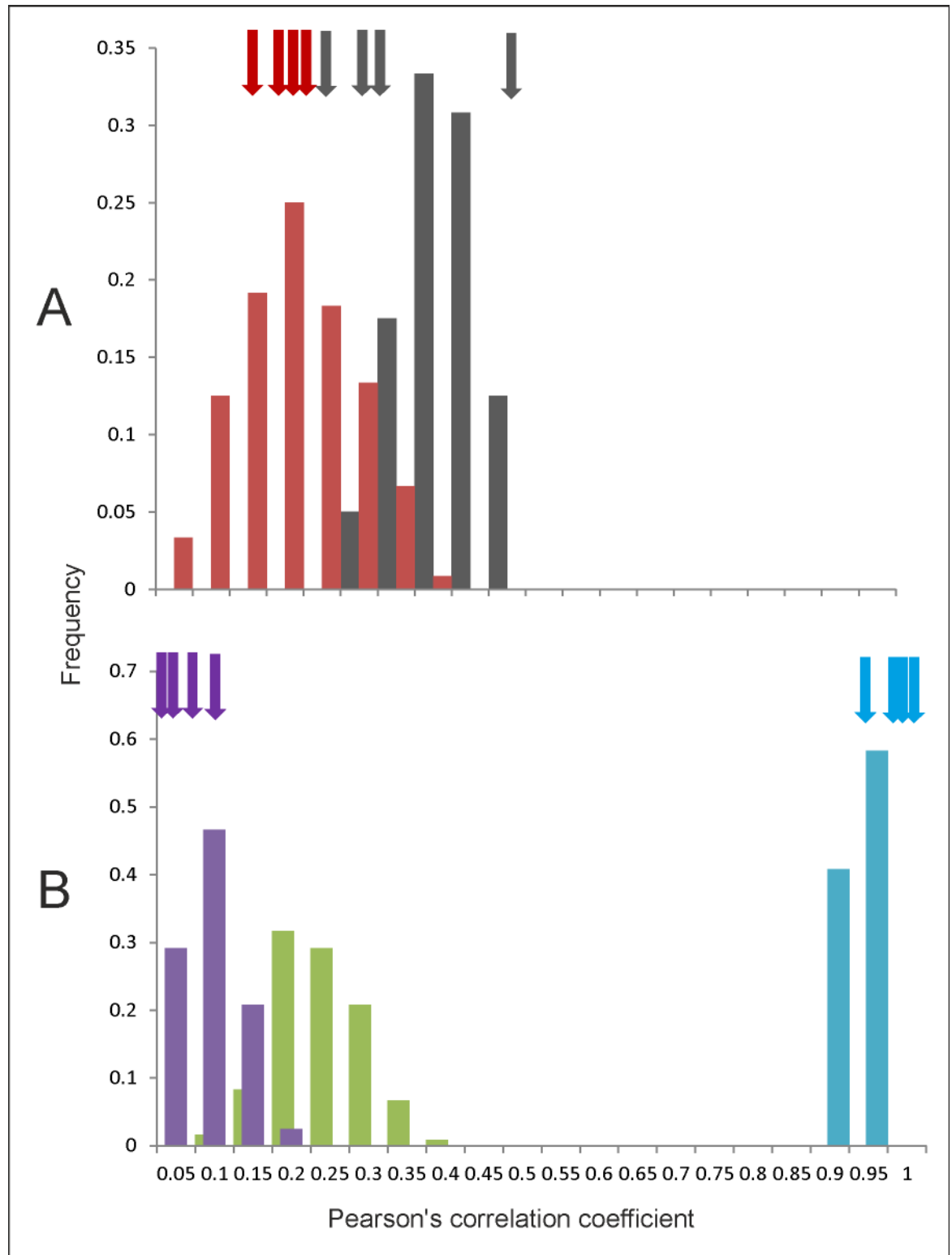


Fig 6. Frequency distribution of correlation coefficients in simulations of the classical pathway leading to prediabetic state: Bars represent the distribution of Pearson's correlations obtained in 10000 runs of simulations. The arrows indicate Pearson's correlations in the four sets of empirical data.

<https://doi.org/10.1371/journal.pone.0204755.g006>

Table 13. Testing the four predictions for the null model, which is a convergent pathway (Fig 5B); A=Glucose, B=HOMA IR, C=Insulin.

Prediction R1 $r^2_{AC} < r^2_{AB} \cdot r^2_{BC}$	CI of r^2_{AC}		CI of $r^2_{AB} \cdot r^2_{BC}$		Accepted/Rejected
	Lower	Upper	Lower	Upper	
CRISIS	0.013	0.081	0.180	0.300	Accepted
KEM PMNS	-0.004	0.082	0.035	0.162	Not rejected
NHP-SA	-0.004	0.057	0.013	0.098	Not rejected
NHP-EU	0.016	0.084	0.050	0.139	Not rejected
Prediction R2 $M_{ca} < M_{ba} \cdot M_{cb}$	CI of M_{ca}		CI of $M_{ba} \cdot M_{cb}$		Accepted/Rejected
	Lower	Upper	Lower	Upper	
CRISIS	-0.053	0.163	0.104	0.146	Accepted
KEM PMNS	-0.185	0.568	0.195	0.413	Accepted
NHP-SA	-0.199	0.611	0.1761	0.418	Accepted
NHP-EU	-0.178	0.548	0.190	0.320	Accepted
Prediction R3 $r_{EbaEcb} > 0$	CI of r_{EbaEcb}				Accepted/Rejected
	Lower	Upper	Lower	Upper	
CRISIS		0.390		0.521	Accepted
PMNS		0.118		0.333	Accepted
NHP-SA		0.081		0.268	Accepted
NHP-EU		0.178		0.328	Accepted
Prediction 4a $r_{EbaC} > r_{BC}$	CI r_{EbaC}		CI r_{BC}		Accepted/Rejected
	Lower	Upper	Lower	Upper	
CRISIS	0.953	0.965	0.918	0.941	Accepted
KEM PMNS	0.966	0.978	0.982	0.988	Rejected
NHP-SA	0.980961	0.987	0.994	0.995	Rejected
NHP-EU	0.968	0.977	0.993	0.995	Rejected

<https://doi.org/10.1371/journal.pone.0204755.t013>

correlation between the two. The r^2 ranges from 0.026 to 0.049, and thus not more than 5% of variance is explained by the relationship.

If we consider FG and FI to be independent and HOMA-IR and HOMA- β derived from them, they constitute a convergent pathway that can be tested by the pathway predictions. It can be seen that predictions from R1, R2 and R3 of the convergent pathway are accepted. However, prediction from R4 and the pathway-specific prediction are rejected (Tables 12 and 13). These rejections can be explained by the positive correlation between FG and FI. We have seen in the analysis of pathway P3 that if A and C are positively correlated then $r^2_{AB} + r^2_{BC}$ can be greater than 1. The rejection of the null model suggests that there is a relationship between FG and FI, but does not indicate whether it comes from the classical pathway or through any other source as in Fig 5C.

7.3.4. Approach 4. If we ignore the non-linearity of the model and assume HOMA-IR and HOMA- β to faithfully represent insulin resistance and beta cell response, we may use the 4 predictions of the standard negative feedback pathway. It is seen that predictions from R1, R2 and R3 are accepted but the outcome of prediction from R4 is complex (Table 14). After correcting for the effect of HOMA-IR, the FG-FI correlation should be weakened and that difference would be predicted by the correlation between HOMA-IR and FG. However instead of weakening, the FG-FI correlation becomes negative. Because of the strong positive correlation between HOMA-IR and FI, correcting for HOMA-IR subtracts from every value of FG, a quantity proportionate to FI, leading to a negative correlation between the corrected FG and FI. Additionally, simulations of the pathway show that if true insulin resistance is assumed to be correlated to FG by the same order as HOMA-IR, the correlation of true insulin resistance

Table 14. Testing the four predictions for a simplified form of the classical negative feedback pathway (Fig 5A); (A= HOMA IR, B=glucose, C=insulin).

Prediction R1 $r^2_{AC} > r^2_{AB} \cdot r^2_{BC}$	CI r^2_{AC}		CI of $r^2_{AB} \cdot r^2_{BC}$		Accepted/Rejected
	Lower	Upper	Lower	Upper	
CRISIS	0.845	0.886	0.003	0.300	Accepted
KEM PMNS	0.9652	0.978	-0.001	0.161	Accepted
NHP-SA	0.988	0.99	-4.8695E-05	0.006	Accepted
NHP-EU	0.986	0.990	0.001	0.012	Accepted
Prediction R2 $M_{ca} > M_{ba} \cdot M_{cb}$	CI M_{ca}		CI of $M_{ba} \cdot M_{cb}$		Accepted/Rejected
	Lower	Upper	Lower	Upper	
CRISIS	-3.242	9.967	0.222	0.641	Accepted
KEM PMNS	0.083	0.299	0.080	0.587	Rejected
NHP-SA	0.085	0.326	0.038	0.334	Accepted
NHP-EU	-3.766	11.581	0.132	0.457	Accepted
Prediction R3 $r_{EbaEcb} < 0$	Lower r_{EbaEcb}		Upper r_{EbaEcb}		Accepted/Rejected
CRISIS		-0.574		-0.452	Accepted
PMNS		-0.414		-0.210	Accepted
NHP-SA		-0.325		-0.142	Accepted
NHP-EU		-0.379		-0.234	Accepted
Prediction R4a $r_{EbaC} < r_{BC}$	CI r_{EbaC}		CI r_{BC}		Accepted/Rejected
	Lower	Upper	Lower	Upper	
CRISIS	-0.392	-0.243	0.136	0.294	Rejected
PMNS	-0.231	-0.008	0.087	0.305	Rejected
NHP-SA	-0.168	0.023	0.068	0.256	Rejected
NHP-EU	-0.167	-0.008	0.145	0.298	Rejected

<https://doi.org/10.1371/journal.pone.0204755.t014>

with FI is far less than that between HOMA-IR and FI (a result similar to Fig 6 and therefore not separately shown). Thus, there is an overfitting rejection of prediction from R1 as well. Rejection of this pathway based on two predictions is due to the unrealistically strong correlation between HOMA-IR and FI, which comes from the calculation of HOMA-IR itself.

We need to examine now to what extent HOMA-IR faithfully represents the true insulin resistance because if it does, the classical pathway certainly gets rejected. This can be examined in the simulations since the true insulin resistance is an input variable and HOMA-IR can be calculated as an outcome of the simulations. We see that HOMA-IR is correlated well with true insulin resistance when both e_1 and e_2 are close to zero (Fig 7). As the errors increase, the correlation becomes weaker. In the data, we do not have access to e_1 and e_2 but since the FG-FI correlation also becomes weaker with e_2 , we can look at how HOMA-IR represents true insulin resistance at different levels of FG-FI correlation. It can be seen that as FG-FI correlation becomes weak, HOMA-IR correlation with the true insulin resistance also becomes weak (Fig 7), but this relationship is affected by e_1 . When e_1 is close to zero, i.e. almost all the variation in FG is explained by variation in true insulin resistance, even at low FG-FI correlation, HOMA-IR represents true insulin resistance fairly well, their correlation ranging between 0.58 and 0.7. On the other hand if we assume e_1 to be large i.e. most of the variation in FG is due to random error or effects independent of insulin action, HOMA-IR is poorly correlated with true insulin resistance, the correlation coefficient declining to 0.2. Thus if we assume that the variance in FG is mainly caused by insulin resistance, then we have to reject the classical pathway leading to hyperinsulinemia. Alternatively, it is likely that the classical pathway is true but HOMA-IR does not represent true insulin resistance and that most of the variation in FG is not caused by insulin resistance. The substantially lower than expected slope of the FG-FI

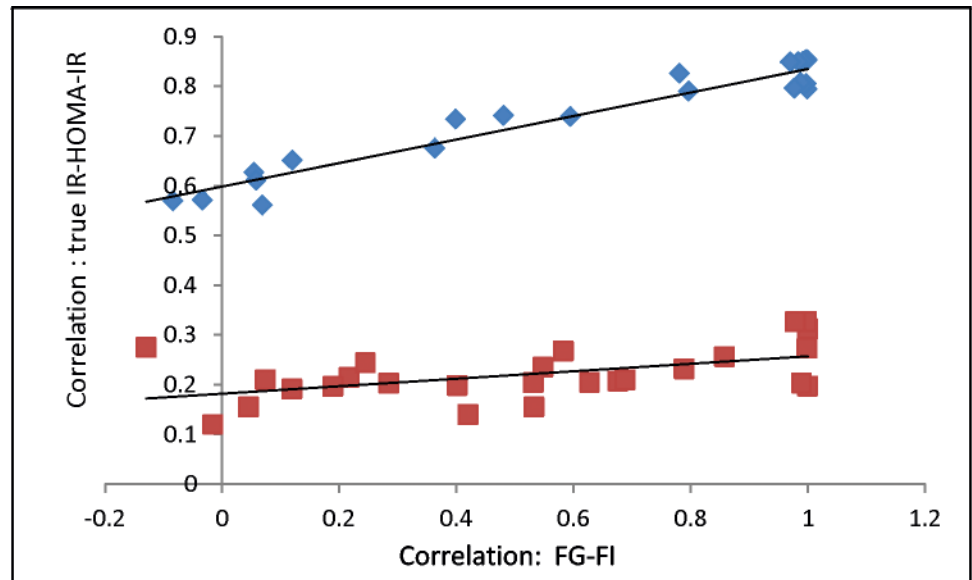


Fig 7. The reliability of HOMA-IR as an index of true insulin resistance. The pathway simulations were carried out at a standard deviation of $e_1=1$ (blue dots) and 10 (red dots). The FG-FI correlation weakens with increase in e_2 which also affects the correlation between true IR and HOMA-IR. It can be seen that HOMA-IR is a reliable indicator of insulin resistance when e_1 is small, but at large e_1 it is a poor indicator as suggested by a weak correlation with true insulin resistance.

<https://doi.org/10.1371/journal.pone.0204755.g007>

regression suggests large random errors in FG making the second interpretation more likely. In any case the classical pathway and the faithfulness of HOMA indices cannot be simultaneously true, and we have to reject at least one of them.

Results of the four alternative approaches to analyze the classical pathway and the null model converge on the inference that the null model is rejected on the basis of a weak but significant correlation between FG and FI. But the weak correlation in FG and FI is not adequately explained by the classical pathway owing to multiple mismatches and rejection of many of its predictions. The pathway rejection may be partially saved by saying that HOMA-IR and HOMA- β are not good indicators of insulin resistance and beta cell response and that we do not have access to true insulin resistance to test the predictions. However the FG-FI regression slope also has a large mismatch with expectations derived from the variance in FI as well as from empirical estimates of K_3 and d . Therefore, it seems more likely that FG and FI are related by causes other than the classical pathway, and HOMA-IR and HOMA- β are derived artificial constructs that do not represent any real life phenomena.

There are a number of real life interpretations of the pathway in Fig 5C. Autonomic inputs from the nervous system are known to affect both insulin secretion and liver glucose production, which might be represented by the common cause arrows of Fig 5C. Alternatively, a small error in data collection can also result in the observed FG-FI correlation. The fasting sampling is done by instructing the subjects to have no food or drink after the last evening meal. However, if even a small proportion of subjects happen to consume bed tea an hour or two before sampling, their glucose as well as insulin levels could be slightly elevated simultaneously. This can result in a weak positive correlation between FG and FI in the data. Since the fasting state is based on the honesty of the subjects and there is no independent monitoring, this source of error cannot be ignored. Thus, there are more than one possible reasons for external factors causing a weak correlation between FG and FI, and the correlation is not sufficient to support the classical pathway in the presence of multiple other mismatches.

It should be noted that the correlational patterns in the four data sets used are remarkably similar although they come from populations differing in location, ethnicity and culture. It would be important to see whether the same correlational patterns are observed in other populations as well, but we can be confident in rejecting the classical pathway at least in the populations sampled.

7.4. What can type 2 diabetes research gain from our analysis

Putting the results together, it can safely be concluded that HOMA-IR and HOMA- β appear to be artificial constructs and reflect very marginally, if at all, the true insulin resistance and β cell response in a steady state. Before our approach for testing a causal pathway was available, there was no way to test whether HOMA-IR and HOMA- β truly represent the intended states of the system. Because of this limitation, insulin resistance was a circular argument. The inability of insulin to regulate glucose was assumed to be because of insulin resistance, but insulin resistance was measured as the inability of insulin to regulate glucose. This circularity had made the hypothesis of insulin resistance and compensatory hyperinsulinemia non-falsifiable. Our approach to pathway predictions breaks the circularity, and makes it possible to test whether the insulin resistance and glucose-mediated compensatory hyperinsulinemia hypothesis is supported by epidemiological data. At least in the populations tested, many serious anomalies in the classical pathway leading to a hyperinsulinemic, normoglycemic, insulin resistance prediabetic state are exposed. Conservatively we can argue that since HOMA-IR and HOMA- β do not represent insulin resistance and β cell response faithfully, and we do not have alternative measures for them, it may not be possible to clearly reject the classical pathway, but the data clearly show that even if true, the classical pathway has a very limited role in deciding FG, FI and their inter-relationship. Both the steady state levels have a large component of error or effects independent of the pathway under consideration. Although our analysis is restricted to the prediabetic state at present, establishing causality in the prediabetic state has implications for the over diabetic state. According to classical thinking, a failure of compensatory insulin response leads to diabetic hyperglycemia. Since our analysis questions the compensatory insulin response itself, the pathway leading to hyperglycemia is also in question. Even a highly conservative inference would demand rethinking of the causal process leading to diabetes.

It should be noted that although the HOMA indices may not reflect what they are intended to reflect, they do not cease to be useful. They may still reflect on the population variability in the glucose and insulin responses and many attempts to analyze this variability and classify diabetes have used the HOMA indices insightfully [40,41]. Therefore although the interpretations might change, the HOMA indices may still serve a useful purpose.

Doubts about the classical pathway are raised independently by experiments using insulin receptor knockouts or insulin suppression. Muscle-specific insulin receptor knockouts show altered glucose tolerance curves but normal fasting insulin [42]. Insulin suppression experiments do not result in elevated fasting glucose [43–45]. Inactivation of insulin degrading enzyme raises steady state insulin levels but does not decrease glucose levels [46,47]. These experiments have already challenged the classical pathway. Thus, there are multiple reasons to doubt the classical pathway. On the other hand, a number of factors other than the mutual effects of FG and FI are known to affect insulin response as well as glucose homeostasis [48–54], but these factors have not been integrated into the mainstream glucose homeostasis models. We do not intend here to test all possible alternative pathways deciding FG and FI. But our study lays down a set of methods by which this can be done, once the pathway hypotheses are clearly spelt out and the causal variables are measured. An important contribution of our methods is that physiological causal pathways can be evaluated based on epidemiological data,

which is potentially a very important tool in understanding complex disorders. Experimental biology reveals what *can* happen in a system, but what *does* happen at the population level is better revealed by epidemiological data. Therefore, discerning causal signatures of pathophysiological pathways in epidemiological data is likely to be an important breakthrough.

8. Conclusions

Making causal inferences from cross sectional correlational data is a long-standing problem. A correlation between two variables does not give reliable information about causal relations. However, we demonstrate here, in the context of steady state homeostatic systems, using mathematical proofs as well as simulations from causal pathways that, in a set of three or more correlated variables, it is possible to test causal hypotheses based on the interrelationships of regression-correlation parameters. This is potentially a highly valuable tool in making causal inferences from cross sectional data in several fields.

Using this set of principles, we tested the classical causal assumption behind the hyperinsulinemic, normoglycemic, insulin resistant or pre-diabetic state. The analysis showed that this causal pathway and the measures of insulin resistance and insulin response were not supported by epidemiological data. Thus, the objections raised recently to the classical causal pathway are validated and alternative causal pathways that already have substantial experimental evidence need to be integrated in the mainstream clinical thinking.

Supporting information

S1 Text. Deriving predictions for regression parameters based on causal equations and calculation of causal parameters for simulations.

(DOCX)

S2 Text. Empirical estimates for parameters used in simulations.

(DOCX)

Acknowledgments

We thank Chittaranjan Yajnik for making the CRISIS and PMNS data sets available to us. We would also like to thank Louise Hayes and Raj Bhopal for making the data from NHP studies available. We thank Subhash Lele and Anil Gore for useful comments on an earlier draft manuscript.

Author Contributions

Conceptualization: Anagha Pund, Milind Watve.

Data curation: Anagha Pund, Shubhankar Kulkarni, Manawa Diwekar-Joshi.

Formal analysis: Suraj Chawla, Vibishan B.

Software: Vibishan B.

Supervision: Milind Watve.

Visualization: Milind Watve.

Writing – original draft: Milind Watve.

Writing – review & editing: Manawa Diwekar-Joshi, Milind Watve.

References

1. Parascandola M, Weed DL. Causation in epidemiology. *J Epidemiol Community Health*. 2001; 55(12):905–12. <https://doi.org/10.1136/jech.55.12.905> PMID: 11707485
2. Gerber JS, Offit PA. Vaccines and Autism: A Tale of Shifting Hypotheses. *Clin Infect Dis* [Internet]. 2009 Feb 15; 48(4):456–61. Available from: <https://academic.oup.com/cid/article-lookup/doi/10.1086/596476> <https://doi.org/10.1086/596476> PMID: 19128068
3. Ratzan SC. Setting the Record Straight: Vaccines, Autism, and the Lancet. *J Health Commun* [Internet]. 2010 Apr 30; 15(3):237–9. Available from: <http://www.tandfonline.com/doi/abs/10.1080/10810731003780714> <https://doi.org/10.1080/10810731003780714> PMID: 20432106
4. Ejima K, Li P, Smith DL, Nagy TR, Kadish I, van Groen T, et al. Observational research rigour alone does not justify causal inference. *Eur J Clin Invest* [Internet]. 2016 Dec; 46(12):985–93. Available from: <http://doi.wiley.com/10.1111/eci.12681> <https://doi.org/10.1111/eci.12681> PMID: 27711975
5. Hill AB. The Environment and Disease: Association or Causation? *Proc R Soc Med*. 1965 May; 58(5):295–300.
6. Meehl PE, Waller NG. The path analysis controversy: a new statistical approach to strong appraisal of verisimilitude. *Psychol Methods* [Internet]. 2002 Sep; 7(3):283–300. Available from: <http://www.ncbi.nlm.nih.gov/pubmed/12243300> PMID: 12243300
7. Niles HE. The Method of Path Coefficients an Answer to Wright. *Genetics* [Internet]. 1923 May; 8(3):256–60. Available from: <http://www.ncbi.nlm.nih.gov/pubmed/17246012> PMID: 17246012
8. Wright S. The Method of Path Coefficients. *Ann Math Stat* [Internet]. 1934 Sep; 5(3):161–215. Available from: <http://projecteuclid.org/euclid.aoms/1177732676>
9. Wright S. Path Coefficients and Path Regressions: Alternative or Complementary Concepts? *Bio-metrics* [Internet]. 1960 Jun; 16(2):189. Available from: <http://www.jstor.org/stable/2527551?origin=crossref>
10. Greenland S. An introduction to instrumental variables for epidemiologists. *Int J Epidemiol* [Internet]. 2000 Aug; 29(4):722–9. Available from: <https://academic.oup.com/ije/article-lookup/doi/10.1093/ije/29.4.722> PMID: 10922351
11. Granger CWJ. Investigating Causal Relations by Econometric Models and Cross-spectral Methods. *Econometrica* [Internet]. 1969 Aug; 37(3):424. Available from: <http://www.jstor.org/stable/1912791?origin=crossref>
12. Rosenbaum PR, Rubin DB. The central role of the propensity score in observational studies for causal effects. *Biometrika* [Internet]. 1983; 70(1):41–55. Available from: <https://academic.oup.com/biomet/article-lookup/doi/10.1093/biomet/70.1.41>
13. Peters J, Janzing D, Scholkopf B. Causal Inference on Discrete Data Using Additive Noise Models. *IEEE Trans Pattern Anal Mach Intell*. 2011 Dec; 33(12):2436–50. <https://doi.org/10.1109/TPAMI.2011.71> PMID: 21464504
14. Neuberger LG. CAUSALITY: MODELS, REASONING, AND INFERENCE, by Judea Pearl, Cambridge University Press, 2000. *Econom Theory* [Internet]. 2003 Aug 6; 19(04). Available from: http://www.journals.cambridge.org/abstract_S0266466603004109
15. Pearl J. Causal inference in statistics: An overview. *Stat Surv* [Internet]. 2009; 3:96–146. Available from: <http://projecteuclid.org/euclid.ssu/1255440554>
16. Peters J, Janzing D, Scholkopf B. Causal Inference on Discrete Data Using Additive Noise Models. *IEEE Trans Pattern Anal Mach Intell* [Internet]. 2011 Dec; 33(12):2436–50. Available from: <http://ieeexplore.ieee.org/document/5740928/> <https://doi.org/10.1109/TPAMI.2011.71> PMID: 21464504
17. Peters J, Mooij JM, Janzing D, Schölkopf B. Causal Discovery with Continuous Additive Noise Models. *J Mach Learn Res*. 2014; 15:2009–53.
18. Eichler M. Causal inference with multiple time series: principles and problems. *Philos Trans R Soc A Math Phys Eng Sci* [Internet]. 2013 Jul 15; 371(1997):20110613–20110613. Available from: <http://rsta.royalsocietypublishing.org/cgi/doi/10.1098/rsta.2011.0613>
19. Abdul-Ghani MA, Tripathy D, DeFronzo RA. Contributions of beta-cell dysfunction and insulin resistance to the pathogenesis of impaired glucose tolerance and impaired fasting glucose. *Diabetes Care* [Internet]. 2006 May; 29(5):1130–9. Available from: <http://www.ncbi.nlm.nih.gov/pubmed/16644654> <https://doi.org/10.2337/diacare.2951130> PMID: 16644654
20. Cerf ME. Beta Cell Dysfunction and Insulin Resistance. *Front Endocrinol (Lausanne)* [Internet]. 2013; 4. Available from: <http://journal.frontiersin.org/article/10.3389/fendo.2013.00037/abstract>
21. Watve M. *Doves, Diplomats, and Diabetes* [Internet]. New York, NY: Springer New York; 2013. Available from: <http://link.springer.com/10.1007/978-1-4614-4409-1>

22. Dubuc PU. The development of obesity, hyperinsulinemia, and hyperglycemia in ob/ob mice. *Metabolism* [Internet]. 1976 Dec; 25(12):1567–74. Available from: <http://www.ncbi.nlm.nih.gov/pubmed/994838> PMID: 994838
23. Dubuc PU. Non-essential role of dietary factors in the development of diabetes in ob/ob mice. *J Nutr* [Internet]. 1981 Oct; 111(10):1742–8. Available from: <http://www.ncbi.nlm.nih.gov/pubmed/7026742> <https://doi.org/10.1093/jn/111.10.1742> PMID: 7026742
24. Garvey WT, Olefsky JM, Marshall S. Insulin induces progressive insulin resistance in cultured rat adipocytes. Sequential effects at receptor and multiple postreceptor sites. *Diabetes* [Internet]. 1986 Mar; 35(3):258–67. Available from: <http://www.ncbi.nlm.nih.gov/pubmed/3512337> PMID: 3512337
25. Shanik MH, Xu Y, Skrha J, Dankner R, Zick Y, Roth J. Insulin Resistance and Hyperinsulinemia: Is hyperinsulinemia the cart or the horse? *Diabetes Care* [Internet]. 2008 Feb 1; 31(Supplement 2):S262–8. Available from: <http://care.diabetesjournals.org/cgi/doi/10.2337/dc08-s264>
26. Corkey BE. Banting lecture 2011: hyperinsulinemia: cause or consequence? *Diabetes* [Internet]. 2012 Jan; 61(1):4–13. Available from: <http://www.ncbi.nlm.nih.gov/pubmed/22187369> <https://doi.org/10.2337/db11-1483> PMID: 22187369
27. Lerner RL, Porte D. Acute and steady-state insulin responses to glucose in nonobese diabetic subjects. *J Clin Invest* [Internet]. 1972 Jul 1; 51(7):1624–31. Available from: <http://www.jci.org/articles/view/106963> <https://doi.org/10.1172/JCI106963> PMID: 4555783
28. Turner RC, Holman RR, Matthews D, Hockaday TD, Peto J. Insulin deficiency and insulin resistance interaction in diabetes: estimation of their relative contribution by feedback analysis from basal plasma insulin and glucose concentrations. *Metabolism* [Internet]. 1979 Nov; 28(11):1086–96. Available from: <http://www.ncbi.nlm.nih.gov/pubmed/386029> PMID: 386029
29. Halter JB, Ward WK, Porte D, Best JD, Pfeifer MA. Glucose regulation in non-insulin-dependent diabetes mellitus. Interaction between pancreatic islets and the liver. *Am J Med* [Internet]. 1985 Aug 23; 79(2B):6–12. Available from: <http://www.ncbi.nlm.nih.gov/pubmed/2863979> PMID: 2863979
30. Matthews DR, Hosker JP, Rudenski AS, Naylor BA, Treacher DF, Turner RC. Homeostasis model assessment: insulin resistance and β -cell function from fasting plasma glucose and insulin concentrations in man. *Diabetologia* [Internet]. 1985 Jul; 28(7):412–9. Available from: <http://link.springer.com/10.1007/BF00280883> PMID: 3899825
31. Fuller WA, editor. *Measurement Error Models* [Internet]. Hoboken, NJ, USA: John Wiley & Sons, Inc.; 1987. (Wiley Series in Probability and Statistics). Available from: <http://doi.wiley.com/10.1002/9780470316665>
32. Griggs RC, Kingston W, Jozefowicz RF, Herr BE, Forbes G, Halliday D. Effect of testosterone on muscle mass and muscle protein synthesis. *J Appl Physiol* [Internet]. 1989 Jan; 66(1):498–503. Available from: <http://www.ncbi.nlm.nih.gov/pubmed/2917954> <https://doi.org/10.1152/jappl.1989.66.1.498> PMID: 2917954
33. Kraemer WJ, Ratamess NA. Hormonal responses and adaptations to resistance exercise and training. *Sports Med* [Internet]. 2005; 35(4):339–61. Available from: <http://www.ncbi.nlm.nih.gov/pubmed/15831061> PMID: 15831061
34. Cumming DC, Brunsting LA, Strich G, Ries AL, Rebar RW. Reproductive hormone increases in response to acute exercise in men. *Med Sci Sports Exerc* [Internet]. 1986 Aug; 18(4):369–73. Available from: <http://www.ncbi.nlm.nih.gov/pubmed/2943968> PMID: 2943968
35. Tomasi T, Sledz D, Wales JK, Recant L. Insulin half-life in normal and diabetic subjects. *Rev Neuropsychiatr Infant* [Internet]. 1966 Dec; 14(12):315–7. Available from: <http://www.ncbi.nlm.nih.gov/pubmed/5988016> PMID: 5988016
36. Pories WJ, Dohm GL. Diabetes: Have We Got It All Wrong?: Hyperinsulinism as the culprit: surgery provides the evidence. *Diabetes Care* [Internet]. 2012 Dec 1; 35(12):2438–42. Available from: <http://care.diabetesjournals.org/cgi/doi/10.2337/dc12-0684> <https://doi.org/10.2337/dc12-0684> PMID: 23173133
37. Yajnik CS, Joglekar C V, Lubree HG, Rege SS, Naik SS, Bhat DS, et al. Adiposity, inflammation and hyperglycaemia in rural and urban Indian men: Coronary Risk of Insulin Sensitivity in Indian Subjects (CRISIS) Study. *Diabetologia* [Internet]. 2008 Jan; 51(1):39–46. Available from: <http://www.ncbi.nlm.nih.gov/pubmed/17972060> <https://doi.org/10.1007/s00125-007-0847-1> PMID: 17972060
38. Joshi NP, Kulkarni SR, Yajnik CS, Joglekar C V., Rao S, Coyaji KJ, et al. Increasing maternal parity predicts neonatal adiposity: Pune Maternal Nutrition Study. *Am J Obstet Gynecol*. 2005; 193(3):783–9.
39. Bhopal R, Unwin N, White M, Yallop J, Walker L, Alberti KGMM, et al. Heterogeneity of coronary heart disease risk factors in Indian, Pakistani, Bangladeshi, and European origin populations: cross sectional study. *BMJ* [Internet]. 1999 Jul 24; 319(7204):215–20. Available from: <http://www.bmj.com/cgi/doi/10.1136/bmj.319.7204.215> PMID: 10417082
40. Ahlqvist E, Storm P, Käräjämäki A, Martinell M, Dorkhan M, Carlsson A, et al. Novel subgroups of adult-onset diabetes and their association with outcomes: a data-driven cluster analysis of six variables.

- Lancet Diabetes Endocrinol [Internet]. 2018 May; 6(5):361–9. Available from: <https://linkinghub.elsevier.com/retrieve/pii/S2213858718300512> [https://doi.org/10.1016/S2213-8587\(18\)30051-2](https://doi.org/10.1016/S2213-8587(18)30051-2) PMID: 29503172
41. Bellatorre A, Jackson SH, Choi K. Development of the diabetes typology model for discerning Type 2 diabetes mellitus with national survey data. Li D, editor. PLoS One [Internet]. 2017 Mar 2; 12(3): e0173103. Available from: <http://dx.plos.org/10.1371/journal.pone.0173103> <https://doi.org/10.1371/journal.pone.0173103> PMID: 28253317
 42. Kadowaki T. Insights into insulin resistance and type 2 diabetes from knockout mouse models. J Clin Invest [Internet]. 2000 Aug 15; 106(4):459–65. Available from: <http://www.jci.org/articles/view/10830> <https://doi.org/10.1172/JCI10830> PMID: 10953020
 43. Gill G V., Rauf O, MacFarlane IA. Diazoxide treatment for insulinoma: a national UK survey. Postgrad Med J [Internet]. 1997 Oct 1; 73(864):640–1. Available from: <http://pmj.bmj.com/cgi/doi/10.1136/pgmj.73.864.640> PMID: 9497974
 44. Alemzadeh R, Karlstad MD, Tushaus K, Buchholz M. Diazoxide enhances basal metabolic rate and fat oxidation in obese Zucker rats. Metabolism [Internet]. 2008 Nov; 57(11):1597–607. Available from: <http://linkinghub.elsevier.com/retrieve/pii/S0026049508002382> <https://doi.org/10.1016/j.metabol.2008.06.017> PMID: 18940400
 45. Alemzadeh R, Tushaus KM. Modulation of Adipoinular Axis in Prediabetic Zucker Diabetic Fatty Rats by Diazoxide. Endocrinology [Internet]. 2004 Dec; 145(12):5476–84. Available from: <https://academic.oup.com/endo/article-lookup/doi/10.1210/en.2003-1523> <https://doi.org/10.1210/en.2003-1523> PMID: 15319354
 46. Maianti JP, McFedries A, Foda ZH, Kleiner RE, Du XQ, Leissring MA, et al. Anti-diabetic activity of insulin-degrading enzyme inhibitors mediated by multiple hormones. Nature [Internet]. 2014 Jul 21; 511(7507):94–8. Available from: <http://www.nature.com/articles/nature13297> <https://doi.org/10.1038/nature13297> PMID: 24847884
 47. Abdul-Hay SO, Kang D, McBride M, Li L, Zhao J, Leissring MA. Deletion of insulin-degrading enzyme elicits antipodal, age-dependent effects on glucose and insulin tolerance. PLoS One [Internet]. 2011; 6(6):e20818. Available from: <http://www.ncbi.nlm.nih.gov/pubmed/21695259> <https://doi.org/10.1371/journal.pone.0020818> PMID: 21695259
 48. Polgreen LE, Jacobs DR, Nathan BM, Steinberger J, Moran A, Sinaiko AR. Association of Osteocalcin With Obesity, Insulin Resistance, and Cardiovascular Risk Factors in Young Adults. Obesity [Internet]. 2012 Nov; 20(11):2194–201. Available from: <http://doi.wiley.com/10.1038/oby.2012.108> <https://doi.org/10.1038/oby.2012.108> PMID: 22573135
 49. Lo C-M, Obici S, Dong HH, Haas M, Lou D, Kim DH, et al. Impaired insulin secretion and enhanced insulin sensitivity in cholecystokinin-deficient mice. Diabetes [Internet]. 2011 Jul; 60(7):2000–7. Available from: <http://www.ncbi.nlm.nih.gov/pubmed/21602512> <https://doi.org/10.2337/db10-0789> PMID: 21602512
 50. Han DH, Hansen PA, Chen MM, Holloszy JO. DHEA treatment reduces fat accumulation and protects against insulin resistance in male rats. J Gerontol A Biol Sci Med Sci [Internet]. 1998 Jan; 53(1):B19–24. Available from: <http://www.ncbi.nlm.nih.gov/pubmed/9467418> PMID: 9467418
 51. Nonogaki K. New insights into sympathetic regulation of glucose and fat metabolism. Diabetologia [Internet]. 2000 May; 43(5):533–49. Available from: <http://www.ncbi.nlm.nih.gov/pubmed/10855527> <https://doi.org/10.1007/s001250051341> PMID: 10855527
 52. Meek TH, Wisse BE, Thaler JP, Guyenet SJ, Matsen ME, Fischer JD, et al. BDNF action in the brain attenuates diabetic hyperglycemia via insulin-independent inhibition of hepatic glucose production. Diabetes [Internet]. 2013 May; 62(5):1512–8. Available from: <http://www.ncbi.nlm.nih.gov/pubmed/23274899> <https://doi.org/10.2337/db12-0837> PMID: 23274899
 53. Holmaeng A, Bjoerntorp P. The effects of testosterone on insulin sensitivity in male rats. Acta Physiol Scand [Internet]. 1992 Dec; 146(4):505–10. Available from: <http://doi.wiley.com/10.1111/j.1748-1716.1992.tb09452.x> <https://doi.org/10.1111/j.1748-1716.1992.tb09452.x> PMID: 1492567
 54. Parton LE, Ye CP, Coppari R, Enriori PJ, Choi B, Zhang C-Y, et al. Glucose sensing by POMC neurons regulates glucose homeostasis and is impaired in obesity. Nature [Internet]. 2007 Sep 29; 449(7159):228–32. Available from: <http://www.nature.com/articles/nature06098> <https://doi.org/10.1038/nature06098> PMID: 17728716